Tiam–Rac signaling mediates trans-endocytosis of ephrin receptor EphB2 and is important for cell repulsion

Thomas N. Gaitanos,* Jorg Koerner,* and Ruediger Klein

Department of Molecules-Signaling-Development, Max Planck Institute of Neurobiology, 82152 Munich-Martinsried, Germany

Ephrin receptors interact with membrane-bound ephrin ligands to regulate contact-mediated attraction or repulsion between opposing cells, thereby influencing tissue morphogenesis. Cell repulsion requires bidirectional trans-endocytosis of clustered Eph–ephrin complexes at cell interfaces, but the mechanisms underlying this process are poorly understood. Here, we identified an actin-regulating pathway allowing ephrinB$^+$ cells to trans-endocytose EphB receptors from opposing cells. Live imaging revealed Rac-dependent F-actin enrichment at sites of EphB2 internalization, but not during vesicle trafficking. Systematic depletion of Rho family GTPases and their regulatory proteins identified the Rac subfamily and the Rac-specific guanine nucleotide exchange factor Tiam2 as key components of EphB2 trans-endocytosis, a pathway previously implicated in Eph forward signaling, in which ephrins act as in trans ligands of Eph receptors. However, unlike in Eph signaling, this pathway is not required for uptake of soluble ligands in ephrinB$^+$ cells. We also show that this pathway is required for EphB2-stimulated contact repulsion. These results support the existence of a conserved pathway for EphB trans-endocytosis that removes the physical tether between cells, thereby enabling cell repulsion.

Introduction

Cell contact–dependent repulsion is an important mechanism to sort and position mixed cell populations, set up tissue boundaries, and guide migrating cells and navigating axons (Batlle and Wilkinson, 2012). The underlying mechanisms that control contact-dependent repulsion are not well understood. The initial complex of a membrane-anchored repellent cue on the guiding cell and its cognate receptor on the responder cell constitutes a physical tether, which needs to be removed from the cell surface to allow efficient cell detachment. Two mechanisms have been described: (1) proteolytic cleavage of the ligand–receptor ectodomains and (2) endocytosis of the ligand–receptor complex (Klein, 2012). Ephrin receptor (Eph) tyrosine kinases and their membrane-bound ephrin ligands have emerged as key players in cell sorting, migration, and tissue remodeling (Klein, 2012; Lisabeth et al., 2013). In the developing nervous system, Eph–ephrin signaling commonly generates a repulsive guidance response by inducing axonal growth cone collapse, important in, for example, formation of motor neuron tracts in the spinal cord and correct retinotopic mapping in the developing eye (Kania and Klein, 2016). Both receptors and ligands comprise two subfamilies: EphAs that preferentially bind glycosylphosphatidylinositol-anchored ephrinAs, and EphBs that preferentially bind transmembrane ephrinBs with some exceptions (Kullander et al., 2001; Qin et al., 2010). The classic model of Eph and ephrin function in opposing cells involves ephrins acting as in trans ligands of Eph receptors, resulting in "forward" signaling. However, Ephrin receptors can also act as ligands for ephrins, termed "reverse" signaling (Klein, 2012). Eph forward signaling often elicits cell repulsion, whereas ephrin reverse signaling causes either cell repulsion or adhesion (Kania and Klein, 2016).

A unique feature of Eph–ephrin signaling is the requirement of higher-order receptor–ligand clusters to induce a response (Himanen et al., 2010; Seiradake et al., 2010; Schaupp et al., 2014). We and others have previously shown that EphB–ephrinB–mediated repulsion involves trans-endocytosis of the entire receptor–ligand cluster, including parts of the surrounding cell membrane into the opposing cell (Marston et al., 2003; Zimmer et al., 2003; Lauterbach and Klein, 2006). Apart from the notion that cell contact–activated ephrinB trans-endocytosis requires the activity of the Rac1 GTPase and actin polymerization in the EphB responder cell, the underlying signaling mechanisms remain unknown. Moreover, the mechanisms governing EphB trans-endocytosis in the opposite direction into the ephrinB responder cell remain unexplored. Previous and ongoing work on the mechanisms of Eph–ephrin endocytosis relied on the activity of artificially clustered, soluble Eph-Fc and ephrin-Fc fusion proteins, which provide a limited understanding of the

*T.N. Gaitanos and J. Koerner contributed equally to this paper.

Correspondence to Ruediger Klein: rklein@neuro.mpg.de; or Thomas N. Gaitanos, tgaitanos@neuro.mpg.de

Abbreviations used: ANOVA, analysis of variance; CME, clathrin-mediated endocytosis; FRET, Förster resonance transfer; GAP, GTPase activating protein; GEF, guanine exchange factor; SE, standard error.

The Rockefeller University Press $30.00
J. Cell Biol. Vol. 214 No. 6 735–752
www.jcb.org/cgi/doi/10.1083/jcb.201512010

signaling networks involved in Eph–ephrin trans-endocytosis (Parker et al., 2004; Yoo et al., 2010). It remains to be investigated if endocytosis of soluble Eph–ephrin ectodomains activates signaling events similar to the engulfment and pinching off of small membrane protrusions from an opposing cell. At least with respect to signaling, significant differences were noted in Eph$^+$ and ephrin$^+$ cells when comparing soluble fusion protein activation to membrane bound Eph-ephrin stimulation (Jørgensen et al., 2009).

Eph-evoked responses, such as cell collapse and repulsion, are mediated by cytoskeletal rearrangements, controlled by the balance between small GTPase activation and inactivation. Rho family GTPases are molecular switches that regulate actin dynamics. RhoA, Rac1, and Cdc42, each titular members of Rho subfamilies, as well as some of their positive (guanine nucleotide exchange factors [GEFs]) and negative (GTPase activating proteins [GAPs]) regulators, have all been implicated in both Eph–ephrin internalization and signaling (Xu and Wilkinson, 2013). Previous work showed that expression of dominant-negative Rac1 or a fragment of the Scar1 protein that delocalized the Arp2/3 complex from the actin cytoskeleton blocked ephrinB trans-endocytosis (Marston et al., 2003). These results suggested that Eph signaling triggered an actin-dependent engulfment pathway that promoted cell repulsion. Other studies using soluble ephrin-Fc fusion proteins implicated the Rac GEFs Vav2 (Cowan et al., 2005) and T-lymphoma invasion and metastasis-inducing protein 1 (Tiam1; Yoo et al., 2010) as well as the Rab5-GEF Rin1 (Deininger et al., 2008) as positive mediators and the SHIP2 lipid phosphatase as an attenuator of ephrin endocytosis into Eph$^+$ cells (Zhuang et al., 2007). Although no study to date has investigated the molecular mechanism of Eph trans-endocytosis into an ephrin responder cell, experiments using soluble Eph-Fc proteins established tentative links to clathrin-mediated endocytosis and the requirement of dynamin (Parker et al., 2004).

Here, we identified components of a pathway that triggers EphB2 trans-endocytosis into ephrinB$^+$ cells. Unlike previous work (Marston et al., 2003), we find F-actin enrichment in ephrinB$^+$ responder cells at the sites of contact and EphB2 internalization. F-actin association with internalized EphB2 is lost when EphB2$^+$ vesicles subsequently traffic into the cytoplasm. We further demonstrate that F-actin enrichment and EphB2 trans-endocytosis require the activity of the Rac subfamily of GTPases. Importantly, Rac activity is not required for uptake of soluble EphB proteins, arguing that the type of mechanism for ephrinB-mediated uptake of EphB critically depends on membrane tethering of EphB. Using the EphB2 trans-endocytosis co-culture assay, we performed a functional siRNA knockdown screen for all Rho family GEFs and GAPs. We identified the Rac-GEF Tiam2 as a key component for EphB2 trans-endocytosis into ephrinB$^+$ cells, whereas Tiam2 was dispensable for internalization of soluble EphB-Fc proteins. These results indicate the presence of a Tiam2–Rac–F-actin pathway activated by cell contact–induced ephrin clustering that removes the physical tether between cells and thereby leads to cell repulsion.

Results

Rac-dependent actin polymerization at sites of EphB2 trans-endocytosis

To visualize actin polymerization during EphB2 trans-endocytosis, we overexpressed LifeAct-mCherry (Riedl et al., 2008; Smyth et al., 2012) in Sloan Kettering neuroblastoma (SKN) cells that endogenously express ephrinB1 and ephrinB2 and performed live-cell imaging after co-culturing with HeLa cells overexpressing EphB2ΔC-GFP/Flag (EphB2ΔC). EphB2ΔC lacks its cytoplasmic domain and cannot trigger endocytosis into the EphB2$^+$ cell. Therefore, all EphB2 clusters are taken up by the opposing ephrinB$^+$ cell (Fig. 1, A and B; Zimmer et al., 2003). Because surface staining on fixed SKN cells revealed that >90% of unattached EphB2 clusters were indeed internalized vesicles (unpublished data), we categorized all of the clusters seen by live imaging as internalized vesicles. From the live imaging (Fig. 1 C), we found that scission of EphB2 clusters occurred in just under half the contact sites observed (Fig. S1 A). These internalization events corresponded with a rapid and localized accumulation of F-actin at sites of contact between the two cells (Fig. 1, C and E; and Video 1). Conversely, the majority of contact sites not exhibiting trans-endocytosis did not show actin enrichment (Fig. 1 F). Surprisingly, once the EphB2 clusters were severed from the donor filopodia and formed vesicles in the SKN cell, they were no longer associated with high levels of F-actin (Fig. 1, C and G, compare time point 1:30 with 4:30 min in C). To analyze if actin polymerization was dependent on Rac activity, we applied the Rac inhibitor EHT1864 to the SKN responder cells before HeLa donor cell seeding and imaging, which resulted in a dramatic increase in the number of contact sites that did not lead to internalization (Fig. S1 B). EHT1864 is a pan Rac subfamily inhibitor (Shutes et al., 2007) and was used at a concentration of 10 µM that showed no cytotoxicity (Fig. S1 C). Inhibition of Rac activity strongly reduced both actin dynamics and the amount of F-actin enrichment at filopodia contact sites (Figs. 1 D and S1 D and Video 2). As in the control condition, filopodia contact sites without polymerized actin failed to internalize EphB2 clusters; however, in the few instances where internalization occurred, we did not see a significant concomitant actin polymerization (Fig. 1, H and I). Collectively, these results demonstrate Rac-dependent spatiotemporal dynamics of actin polymerization in the initial stages of EphB2 trans-endocytosis, whereas subsequent intracellular trafficking of resulting vesicles is not associated with high levels of polymerized actin. Because Rac-dependent actin polymerization was previously linked to ephrinB trans-endocytosis (Marston et al., 2003), these results suggest certain similarities between EphB and ephrinB signaling regarding the actin cytoskeleton during the trans-endocytosis process.

Several Rac subfamily GTPases act redundantly

We next quantified the importance of Rac subfamily GTPases (Heasman and Ridley, 2008) for EphB2 trans-endocytosis. For this, we used Rac siRNA knockdown and treatment with EHT1864. Given the potential for redundancy between different members of the Rac subfamily (Gu et al., 2003; Corbetta et al., 2009), we first determined by RT-PCR which members were expressed in SKN and HeLa cells, both cell lines used extensively throughout this study (Fig. S2 A). We found that SKN cells expressed Rac1, Rac3, and RhoG, and subsequent siRNA experiments were therefore performed on the individual proteins as well as in all combinations. Because HeLa cells expressed four members of the Rac subfamily (including Rac2) and siRNA knockdown of four genes is very inefficient, we only used the Rac inhibitor to block activity. We performed the co-culture assay, depleting members of the Rac subfamily in

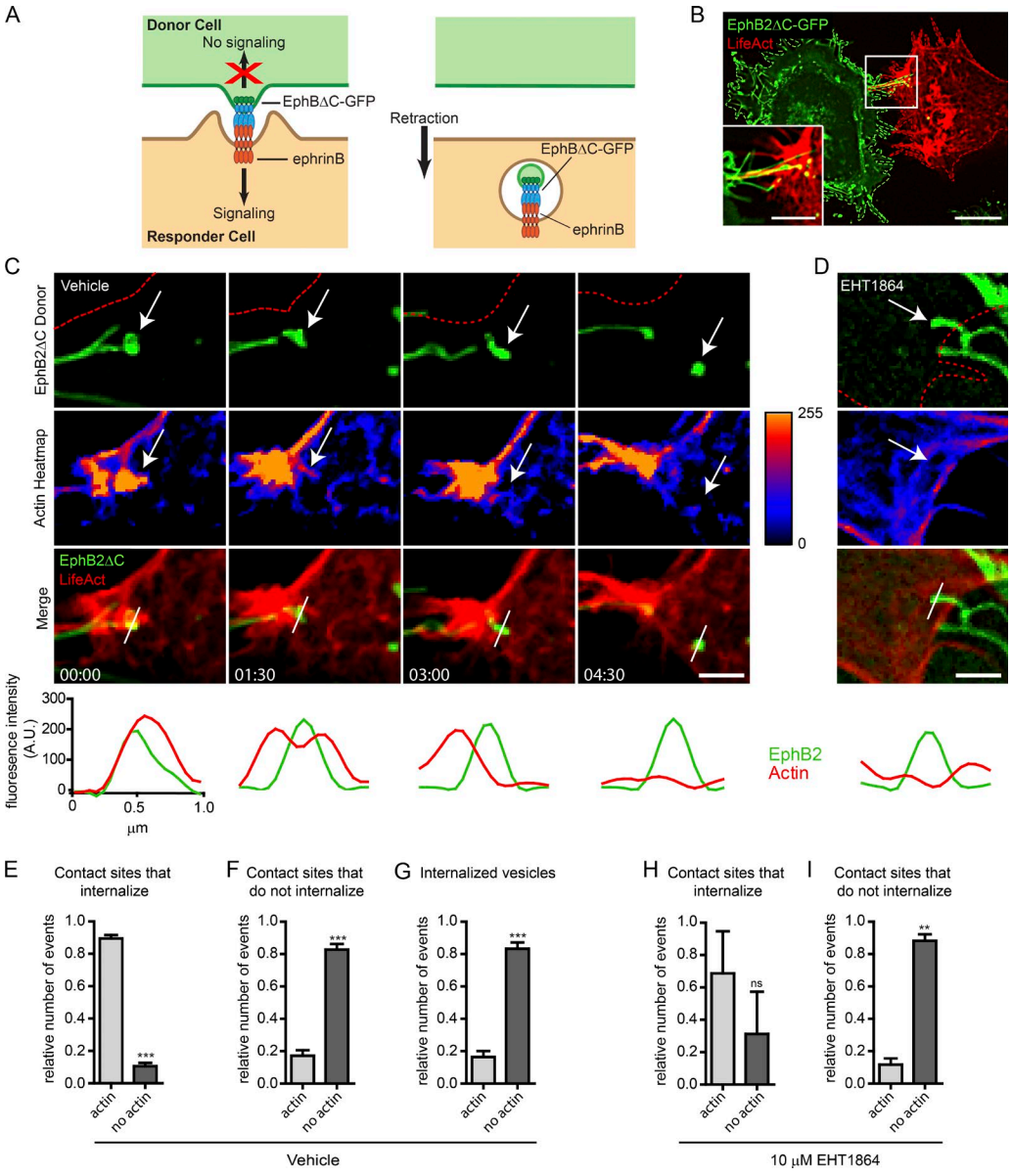

Figure 1. **Rac-dependent actin polymerization during EphB2 trans-endocytosis.** (A) Model of unidirectional EphB2 trans-endocytosis from donor cell into ephrinB$^+$ responder cell. Interaction between ephrinB and signaling-deficient EphBΔC (cytoplasmic domain replaced by GFP) leads to ephrinB–EphB clustering (left) and vesicle formation containing receptor–ligand complexes and donor cell membrane in the ephrinB$^+$ cell (right), enabling cell retraction (Marston et al., 2003; Zimmer et al., 2003). (B) Representative image showing EphB2ΔC-GFP (green) trans-endocytosis into an ephrinB$^+$ SKN cell overexpressing LifeAct-mCherry (red). Cells were co-cultured and imaged live once contact occurred. EphB2ΔC-GFP$^+$ vesicles (green and yellow puncta) can be seen in the SKN cell. Maximum projection of deconvolved images. Bars: 25 µm; (inset) 10 µm. (C and D) Time-lapse images of EphB2ΔC trans-endocytosis into ephrinB$^+$ SKN cells overexpressing LifeAct-mCherry treated with either vehicle (C) or 10 µM EHT1864 (D; only 4-h time point shown, full time series in Fig. S1 D). Cells were co-cultured and images acquired every 90 s. Top row, EphB2 channel (red outline indicates SKN cell border); second row, heatmap for fluorescence intensity from LifeAct channel. Arrow tracks vesicle from contact point to internalization. (Bottom) Line graphs of fluorescence intensity for LifeAct (red curves) and EphB2 (green curves) measured across contact point and subsequent vesicle, as indicated by the white bar in the merge row. Maximum projection of deconvolved images. Bar, 1 µm. Elapsed time shown as minutes:seconds. (E–G) Quantifications from C. Fractions of colocalization of LifeAct with EphB2ΔC-GFP at contact sites that either lead to vesicle formation (E) or do not (F). (G) Fractions of colocalization of LifeAct with internalized EphB2$^+$ vesicles tracked from contact. To ensure proper separation from filopodia, vesicle-actin colocalization was determined 3 min after scission was first observed. Data are presented as mean ± SE (n = 5 independent experiments; 4–10 cells per experiment, each with multiple events recorded); ***, $P < 0.001$, Student's t test. (H and I) Quantifications of D and Fig. S1 B. Similar to analysis described in E and F, except EHT1864-treated responder cells were used. Data represent mean ± SE (n = 3 independent experiments; 9–10 cells per experiment, each with multiple events recorded). ns, not significant; **, $P < 0.01$, Student's t test.

ephrinB$^+$ SKN responder cells before co-seeding with donor EphB2ΔC-GFP/Flag$^+$ HeLa cells. Fixed cells were immunostained against the Flag tag without permeabilization to show surface EphB2 (Fig. 2, A and B). Internalized vesicles solely emit GFP signal, whereas surface clusters costain with Flag. We confirmed that depleting or inhibiting Rac subfamily members did not affect ephrinB expression at the plasma membrane (Fig. S2, B–E). To unbiasedly analyze large amounts of data, we developed a semiautomated high-throughput analysis pipeline using CellProfiler (Fig. 2 A). siRNA knockdown of Rac1,

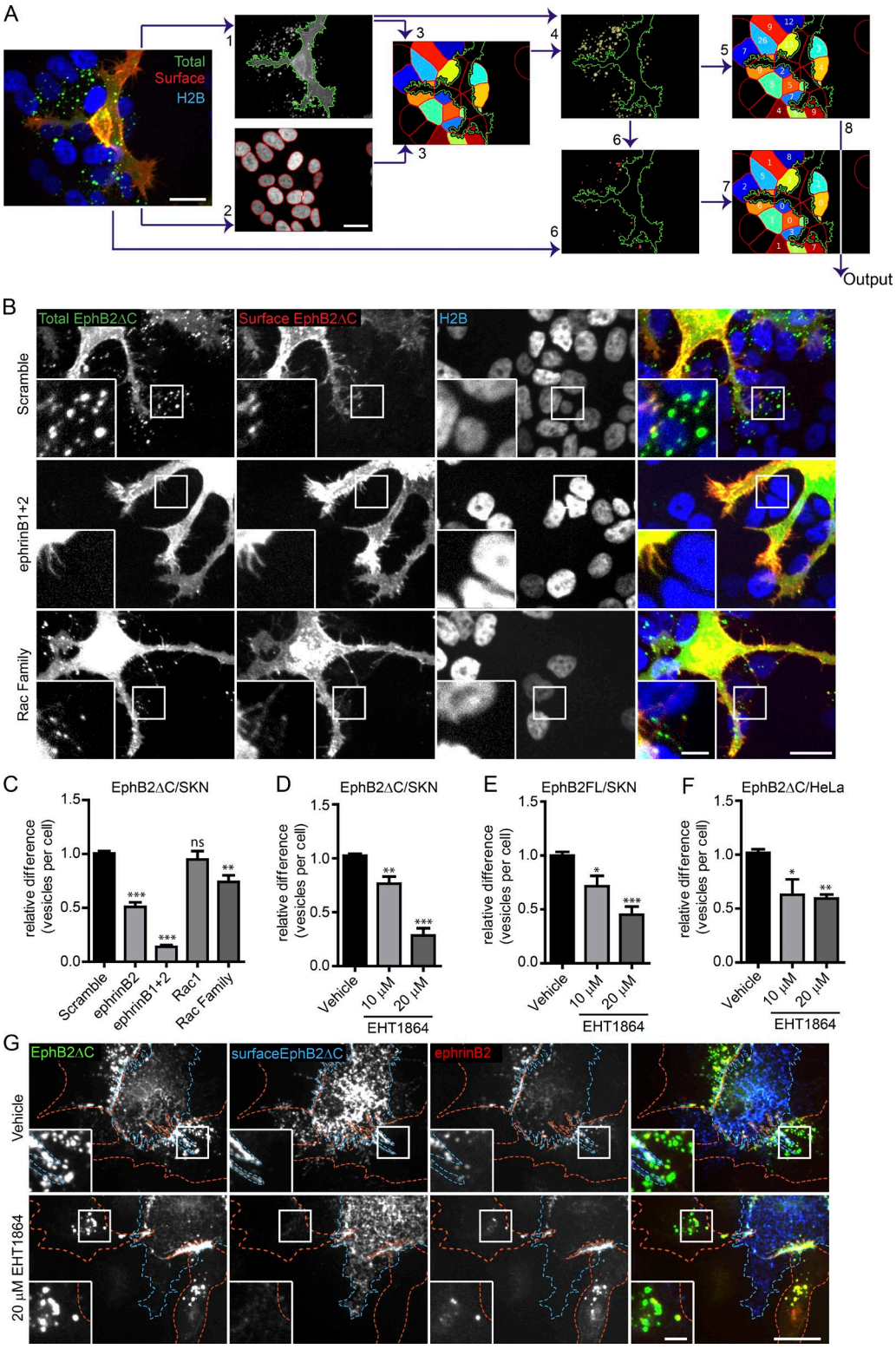

Figure 2. **Rac is required for EphB2ΔC trans-endocytosis into ephrinB⁺ cells.** (A) Selected images highlighting important steps in semiautomated CellProfiler analysis of EphB2ΔC trans-endocytosis into ephrinB⁺ cells. Image acquired from ephrinB⁺ SKN-H2B-RFP cells (responder, shown in blue) co-cultured with EphB2ΔC-GFP/Flag–positive HeLa cells (donor, total EphB2 shown in green). Cells fixed without permeabilization and surface EphB2 labeled with anti-Flag immunostaining (surface EphB2, shown in red). (1) Identification of donor cell in GFP channel, and (2) identification of responder SKN nuclei in RFP channel. (3) SKN cells of interest (colored cells) determined by predicting cell size (50-pixel expansion from SKN nuclei) and restricting to the vicinity (<50 pixels) of the donor cell (green outline). (4) Identification of total vesicles (yellow outline) in total EphB2 channel restricted to SKN cells of interest. (5) Vesicle numbers allocated to individual SKN cell. (6) Identification of surface clusters (red outlines) from surface EphB2 channel restricted to area of total vesicles identified. (7) Surface clusters allocated to individual SKN cell. (8) Number of internalized vesicles per SKN cell (Output) determined by subtracting surface cluster number from total vesicle data. Bars, 20 µm. (B) Representative images showing the effect of Rac1 subfamily depletion on EphB2ΔC trans-endocytosis into ephrinB⁺ SKN cells. SKN cells were treated with siRNA for 72 h before 80 min co-culture with EphB2ΔC-GFP/Flag–positive cells.

Rac3, or RhoG alone, or combinations of pairs of Rac subfamily members, had no effect on EphB2 trans-endocytosis; however, a pool of siRNA oligos targeting all three members expressed in SKN cells significantly reduced the number of internalized vesicles detected (Fig. 2, B and C; and Fig. S2 F). The extent of this reduction (26 ± 6%, mean ± standard error [SE]) was less than when knocking down ephrinB2 alone (49 ± 4%) or in combination with ephrinB1 (86 ± 2%), potentially because of incomplete depletion of Rac subfamily members, in particular when all three proteins were targeted (Fig. S2 G). Overexpression of a Rac1 construct resistant to Rac1 siRNA ($Rac1^r$) in SKN cells depleted of all Rac subfamily members fully rescued the phenotype, further highlighting the requirement of Rac for EphB2 trans-endocytosis, and ruling out off-target effects of the siRNA (Fig. S2 H). In support of this finding, treating SKN cells with EHT1864 also produced a robust dose-dependent reduction in vesicle number compared with vehicle-treated cells (Figs. 2 D and S2 I) or untreated control cells (unpublished data). Importantly, this dose-dependent requirement of Rac activity was also observed when using full-length EphB2-GFP/Flag as a donor molecule (Figs. 2 E and S2 J). These findings confirm that the truncated EphB2 is functionally equivalent to the full-length protein in inducing Rac-dependent trans-endocytosis. Finally, Rac inhibition also blocked EphB2 trans-endocytosis when using HeLa cells overexpressing ephrinB1-mCherry as responder cells (Fig. 2, F and G). These results indicate that the members of the Rac GTPase subfamily mediate EphB2 trans-endocytosis into $ephrinB^+$ cells, and the family members are functionally redundant in this role.

Rac activity is required for EphB2 trans-endocytosis into primary cortical neurons

Trans-endocytosis of EphB receptors into $ephrinB^+$ neurons is crucial for efficient cell detachment during the growth cone collapse response (Zimmer et al., 2003). We therefore wanted to investigate if Rac activity was also required for EphB trans-endocytosis in cultured neurons. Cultures of embryonic day 15.5 (+1 day in vitro) mouse cortical neurons stained with CellTracker green were incubated in the presence of different EHT1864 concentrations or vehicle control before co-culture with EphB2ΔC-mCherry expressing HeLa cells. Live imaging was performed and EphB2 internalization into the neurons at contact sites with HeLa cells was scored (Fig. 3, A and B; and Videos 3 and 4). Treatment of neurons with EHT1864 significantly reduced the extent of EphB2 trans-endocytosis in a dose-dependent manner and prolonged contact between the two cells markedly (not depicted and Videos 3 and 4). We therefore conclude that Rac activity is required for EphB2 trans-endocytosis into primary neurons. Together with the experiments on immortalized cell lines, these results suggest that the requirement of Rac activity for EphB2 trans-endocytosis into $ephrinB^+$ cells represents a general mechanism.

Rac subfamily GTPases are not required for endocytosis of soluble EphB2 ectodomains

With few exceptions (Marston et al., 2003; Zimmer et al., 2003; Lauterbach and Klein, 2006), most studies of Eph-ephrin endocytosis use preclustered soluble ligand or receptor ectodomains to elicit internalization, despite the fact that these proteins are typically membrane bound in vivo (Parker et al., 2004; Cowan et al., 2005; Yoo et al., 2010). Having established the importance of Rac subfamily members for EphB2 trans-endocytosis in a cell–cell context, we next examined whether the same mechanisms were used for endocytosis of soluble EphB ectodomains. We performed the endocytosis assay using EphB2-Fc fusion proteins preclustered with a Cy2-conjugated antibody, as described previously (Davis et al., 1994). Cells were fixed without permeabilization, and surface clusters were immunolabeled (see Materials and methods). Clusters that were present on the surface costained with both fluorophores (which appear as yellow vesicles), whereas vesicles that were internalized only stained for the prelabeled fluorophore (Fig. 4 A, green). CellProfiler-assisted quantification indicated that both depleting Rac1 and its subfamily members by siRNA and the use of the Rac inhibitor failed to block EphB2-Fc endocytosis in SKN cells (Fig. 4, A–C), whereas depletion of ephrinBs produced a marked effect. Treatment with Fc alone showed that endocytosis was dependent on the presence of the EphB2 ectodomain and not on the Fc portion of the fusion protein. These results revealed that Rac subfamily GTPases were not required for reverse endocytosis of soluble EphB2 receptors into SKN cells. Similar results were obtained when using HeLa cells transiently expressing ephrinB1-mCherry (Fig. 4, D and F). HeLa cells also allowed us to compare the results with endocytosis in the opposite direction, namely of soluble ephrinB2 into FL-EphB2-mCherry–expressing cells. Inhibition of Rac indeed blocked uptake of ephrinB2-Fc by EphB2-expressing cells as previously observed (Cowan et al., 2005; Yoo et al., 2010; Um et al., 2014; Fig. 4, E and G). In conclusion, our results indicate that the mechanisms of endocytosis of soluble EphB and ephrinB ectodomains are different; uptake of ephrinB into $EphB^+$ cells requires Rac activity, whereas uptake of EphB into $ephrinB^+$

Cells were fixed without permeabilization and probed against Flag (surface EphB2ΔC, shown in red or yellow in merge). Internalized vesicles appear as green puncta (total EphB2ΔC signal) within the vicinity of the SKN nuclei (H2B channel, shown in blue). Top row, scramble siRNA (negative control); middle row, ephrinB1 and B2 siRNA (positive control); bottom row, Rac1 subfamily siRNA. Image shown as maximum projection. Bars: 20 µm; (inset) 5 µm. (C) Quantification of B. Acquired images were analyzed using CellProfiler. Results shown as mean ± SE (n = 8 independent experiments, >125 responder cells per condition per experiment, vesicle numbers per cell for the indicated siRNAs were normalized to median scramble value per experiment); ns, not significant; *, $P < 0.05$; **, $P < 0.01$; ***, $P < 0.001$, repeated measures one-way ANOVA with Dunnett's post hoc test. (D) Quantification showing the effect of Rac inhibitor EHT1864 versus vehicle control on EphB2ΔC trans-endocytosis into $ephrinB^+$ SKN cells. Results shown as mean ± SE (n = 4 independent experiments, >130 responder cells per condition per experiment); statistics are as described in C. Example images shown in Fig. S2 I. (E) Quantification of the effect of Rac inhibitor EHT1864 versus vehicle control on trans-endocytosis of full-length EphB2 into $ephrinB^+$ SKN cells. Results shown as mean ± SE (n = 7 independent experiments, >40 responder cells per condition per experiment); statistics are as described in C. Example images are shown in Fig. S2 J. Quantification (F) and representative images (G) showing the effect of Rac inhibitor EHT1864 versus vehicle control on EphB2ΔC trans-endocytosis into $ephrinB1^+$ HeLa responder cells. HeLa cells (red outline) overexpressing ephrinB1-mCherry (red puncta where in contact with EphB2, yellow in the merge) were treated for 4 h with either vehicle or EHT1864 at indicated concentrations. Donor cells (blue outline) expressing EphB2ΔC-GFP/Flag (shown in green) were co-cultured with responder cells for 80 min, fixed without permeabilization, and immunostained against Flag (surface EphB2ΔC, shown in blue). Cells were manually scored for internal vesicles. Results shown as mean ± SE (n = 4 independent experiments, 18–61 responder cells per condition per experiment); statistics are as described in C. Bars: 20 µm; (inset) 5 µm.

cells does not. Furthermore, the different mechanisms of ephrinB-mediated uptake of EphB critically depend on whether EphB is membrane tethered or not; trans-endocytosis of membrane-tethered EphB from an opposing cell into the ephrinB$^+$ cell requires Rac activity, whereas uptake of soluble EphB ectodomain into the ephrinB$^+$ cell does not.

EphB2-Fc and ephrinB1-Fc stimulation differentially increase Rac1 activity

Next, we determined whether Rac1 was activated during Eph–ephrin endocytosis. It would have been ideal to measure local Rac activity during Eph–ephrin trans-endocytosis at cell–cell contact sites. However, the fluorophores of the Förster resonance transfer (FRET) sensor RaichuEV-Rac1 (Itoh et al., 2002) were not sufficiently distinct from fluorescently tagged EphB2ΔC constructs to reveal Rac activity near trans-endocytosed EphB2. Instead, we measured Rac activity during uptake of EphB2-Fc and ephrinB1-Fc. HeLa cells overexpressing the Rac1 FRET sensor, with or without coexpression of EphB2 or ephrinB2, were imaged before and after stimulation with fluorescently labeled, preclustered ephrinB1-Fc or EphB2-Fc, respectively (Fig. 4, H, I, and M; and Fig. S3, A–C). Cells expressing the Rac1 FRET sensor only were used as negative controls. Rac1 activity was significantly increased 20 min after stimulation with either ephrinB1-Fc or EphB2-Fc in the cells expressing EphB2 or ephrinB1 as compared with the same time point in control cells lacking EphB2 or ephrinB1 (Fig. 4, J and K). Interestingly, Rac1 activity was sixfold greater in EphB2-expressing cells than ephrinB1-expressing cells, relative to the amount of endocytosis detected, calculated by the total fluorescence intensity of the Fc-protein complexes in the cells (Fig. 4, I, L, and M). These results indicate that in conditions in which Rac1 is required (uptake of soluble ephrinB into EphB$^+$ cells), the increase in Rac activity is highest.

RhoA and Cdc42 subfamilies play a negligible role in EphB2 trans-endocytosis

Having established the role of the Rac subfamily of GTPases in EphB2 trans-endocytosis, we next looked at the RhoA and Cdc42 subfamilies, both of which had previously been implicated in Eph–ephrin signaling and/or endocytosis (Shamah et al., 2001; Irie and Yamaguchi, 2002; Sahin et al., 2005; Nishimura et al., 2006; Takeuchi et al., 2015). The RT-PCR expression profile for SKN and HeLa cells showed the presence of the RhoA subfamily members RhoA and RhoB in both cell lines (Fig. S2 A). RhoA subfamily knockdown did not cause any alteration in EphB2 trans-endocytosis, both in SKN cells and in HeLa cells overexpressing ephrinB2 (Fig. 5, A–C). The knockdown efficiency of RhoA and RhoB was very high (Fig. S4 A), arguing against the possibility of low remaining levels of protein maintaining their function. As with knockdown of the Rac subfamily, expression of ephrinBs at the plasma membrane was not altered after RhoA subfamily members were depleted (Fig. S2, B and D). These results are also in line with previous findings showing that RhoA activity is not elevated in ephrinB-mediated axon retraction (Xu and Henkemeyer, 2009). To analyze the role of RhoA and RhoB in endocytosis of soluble EphB receptors, we knocked down RhoA and RhoB in SKN cells and stimulated them with preclustered EphB2-Fc. This treatment resulted in an up to 1.75-fold increase in the number of internalized vesicles (Figs. 5 D and S4 B), suggesting a role for RhoA subfamily GTPases in negatively regulating uptake of soluble EphB2-Fc.

Finally, we examined the role of the Cdc42 subfamily in EphB2 trans-endocytosis. RT-PCR expression profile for Cdc42 subfamily GTPases showed Cdc42, RhoQ, and RhoU expression in both HeLa and SKN cells (Fig. S2 A). Neither depletion of Cdc42 alone (data not shown) nor depletion of any combination of expressed subfamily members affected EphB trans-endocytosis at cell–cell contacts or uptake of soluble EphB2-Fc in SKN cells (Figs. 5 E and S4 C). Western blotting was performed to ensure the siRNAs were able to specifically deplete their target proteins (Fig. S4, D–F). Collectively, the results so far indicate that trans-endocytosis of membrane-tethered EphB2 from an opposing cell into the ephrinB$^+$ cell requires the activity of Rac, but not RhoA or Cdc42 subfamily GTPases.

A functional siRNA screen for Rho family GEFs and GAPs

Next, we sought to determine how Rho family GTPase activity is regulated during EphB2 trans-endocytosis. To this end, we performed an image-based siRNA screen targeting Rho family GEFs and GAPs in SKN cells (Fig. 6 A). HeLa cells stably expressing EphB2ΔC-GFP were used as donor cells. For every target gene we selected four distinct siRNA oligo sequences, and the entire siRNA library was used twice. In each 96-well imaging plate, 4 wells of scramble siRNA oligos were included as negative controls, and ephrinB2 singularly (3 wells) or in combination with ephrinB1 (2 wells) was depleted as positive controls. Curves showing the number of vesicles per cell illustrated distinct differences among the three control groups (Fig. S5 A). Z-scores were calculated from the scramble siRNAs using mean vesicle cutoff (X) for 40% of the cells for each plate (see Materials and methods). This cutoff produced significant differences among negative controls, ephrinB2 single depletion, and ephrinB1+2 double depletions (Fig. S5 B). Oligos were considered hits when the mean z-scores over both runs were either below −1.25 (reduced endocytosis) or above 1.75 (increased endocytosis; Fig. S5 C). Using these criteria, there were very few false positives (8% of entire scramble siRNA wells) and a very low false negative rate (1% for ephrinB2 single depletion and 0% for ephrinB1+2 double depletion; Fig. S5 D). We annotated all 78 GEFs and 61 GAPs to known GTPase substrates when possible using review articles (Tcherkezian and Lamarche-Vane, 2007; Jaiswal et al., 2013; Cook et al., 2014) and independent literature searches (Fig. 6, B and C; and Table S1). Although GEF and GAP specificity is sometimes ambiguous, GEFs whose siRNA knockdown reduced endocytosis in the assay targeted the Rac subfamily of GTPases (e.g., Rac-specific Tiam2/Stef and the multitargeting Vav1; Fig. 6, B and E; and Table S1). Fittingly, GAPs whose siRNA knockdown increased endocytosis in the assay inhibited Rac activity (DEPDC1B and ARHGAP25) or all subfamilies (OPHN1; Fig. 6 C and Table S1). Conversely, GAPs whose siRNA knockdown reduced endocytosis in the assay mostly regulated RhoA activity (HMHA1, ARHGAP6, and ARHGAP30). The specificity of PIK3R2 (Tcherkezian and Lamarche-Vane, 2007), the second strongest GAP hit, is unknown (Fig. 6 C). Interestingly, the third strongest hit, active breakpoint cluster region-related protein (Abr), which has both GEF and GAP domains for all Rho subfamilies, has previously been implicated in Tiam1-regulated EphB2 signaling in concert with another Rac GAP, breakpoint cluster region-related protein (Um et al., 2014). GEFs whose siRNA knockdown increased vesicle number did not show a clear pattern, including Rho-specific Net1 and Cdc42-specific

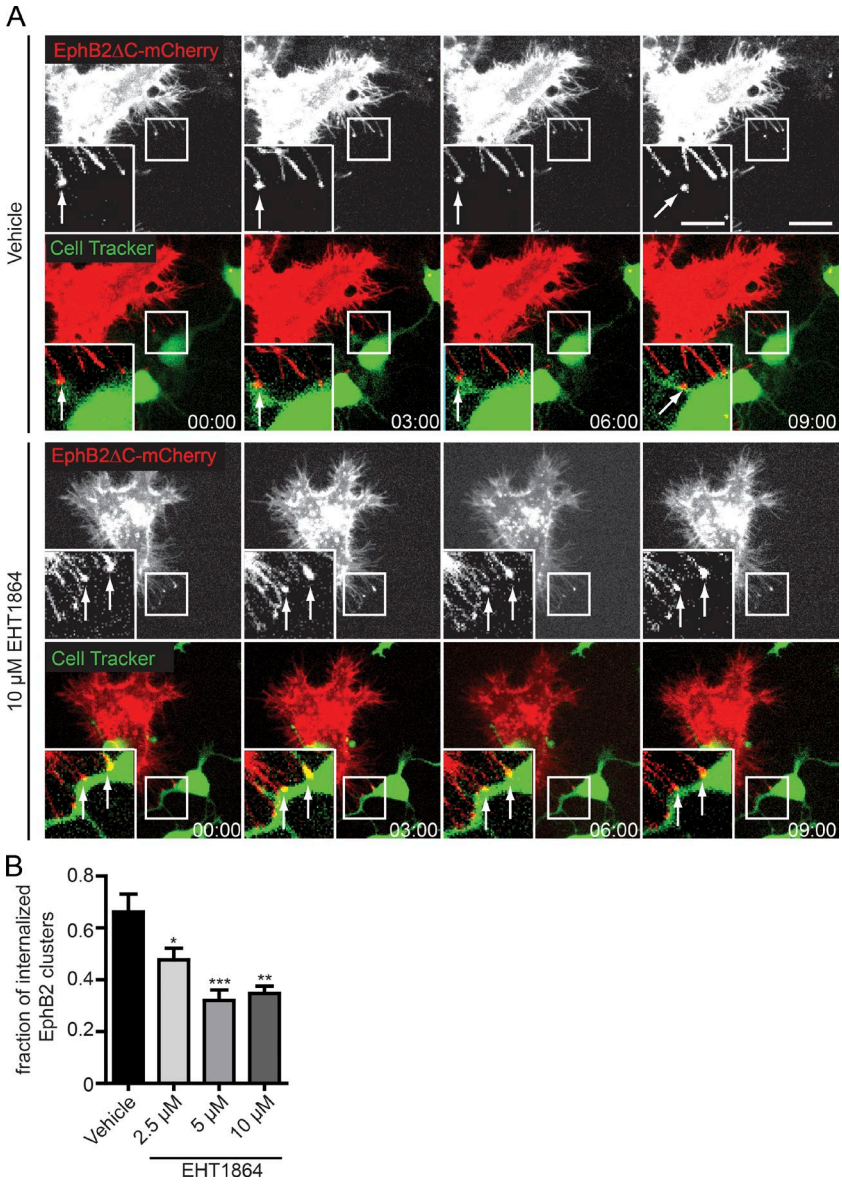

Figure 3. **Rac is required for EphB2ΔC trans-endocytosis into primary neurons.** (A) Representative time course showing the effects of Rac inhibitor EHT1864 versus vehicle control on EphB2ΔC trans-endocytosis into embryonic day 15.5 mouse cortical neurons. At 1 day in vitro, neurons were stained with CellTracker green, treated for 4 h with either vehicle or EHT1864 at the indicated concentrations, and co-cultured with EphB2ΔC-mCherry+ HeLa cells (donor cells, shown in red). Top rows of each condition show donor cell alone, and contact sites and subsequent vesicles are marked by arrows. Time-lapse movies were acquired for 3 h with 3-min intervals between images. Deconvolved image of a single focal plane. Bars: 10 μm; (inset) 5 μm. Elapsed time shown as minutes:seconds. (B) Quantification of A. EphB2 uptake was scored manually from time-lapse images. Results are shown as fraction of contact sites (EphB2 clusters) that resulted in uptake (separated vesicle as seen in last image of top row of A). Data represent mean ± SE (n = 4 independent experiments, 5–12 cells per condition per experiment); *, $P < 0.05$; **, $P < 0.01$; ***, $P < 0.001$, repeated measures one-way ANOVA with Dunnett's post hoc test.

FGD2 and FGD5 (Fig. 6, B and E; and Table S1). In confirmation of the screen, we repeated the knockdown of the two Tiam family members and verified that Tiam2 depletion produced a significant reduction in vesicle numbers (23 ± 6% of control; Fig. 6 D), whereas no effect was seen after Tiam1 depletion. Our screen data support the notion that Rac subfamily members are required for EphB2 trans-endocytosis and implicate, among others, both the Tiam and Vav GEF families as key regulators.

The Rac-GEF Tiam2 is required for both EphB2 and ephrinB1 trans-endocytosis

Because Tiam2 siRNA knockdown was our strongest hit in reducing endocytosis, with all four siRNA oligos scoring below the cutoff of −1.25, we sought to verify its role in EphB2 trans-endocytosis. Western blots confirmed the knockdown of Tiam2 in both HeLa and SKN cells (Fig. S5 E). Confirmation experiments knocking down Tiam2 in HeLa cells overexpressing ephrinB1 cells produced similar results as in naive SKN cells, reducing EphB2 trans-endocytosis by 32 ± 11% (mean ± SE) compared with the controls (Fig. 7, A and B). Moreover, depletion of Tiam2 also reduced vesicle uptake in the opposite direction (47 ± 10% of control), i.e., ephrinB1 trans-endocytosis, using HeLa cells overexpressing EphB2 as responder cells (Fig. 7, A and C). In contrast, knockdown of Tiam2 failed to significantly reduce uptake of soluble EphB2-Fc in SKN cells (Fig. S5 G), suggesting that Rac activity is not required for this process. To test for a Tiam2 gain-of-function phenotype, we used a GFP-tagged, truncated, and thereby constitutively active version of Tiam2 (Tiam2ΔN; Rooney et al., 2010; Fig. S5 H) that still possesses the ephrinB-binding motif (Terawaki et al., 2010). Co-culture of Tiam2ΔN+ SKN cells with EphB2-mCherry donor cells led to a robust increase in EphB2 trans-endocytosis as compared with SKN cells solely expressing GFP (206 ± 15%; Fig. 7, D and E). Conversely, and in accordance with the Tiam2 knockdown results, overexpressing a dominant-negative mutant version of Tiam2ΔN lacking its GEF activity (Tiam2ΔNDN) in SKN cells reduced EphB2 trans-endocytosis as compared with GFP-expressing control cells (Fig. 7, D and E). Furthermore, by overexpressing Tiam2ΔN, we were able to completely rescue the reduction of EphB2 trans-endocytosis after Tiam2 depletion by siRNA. This condition resulted in an increase in the number of vesicles above the GFP-expressing control cells comparable

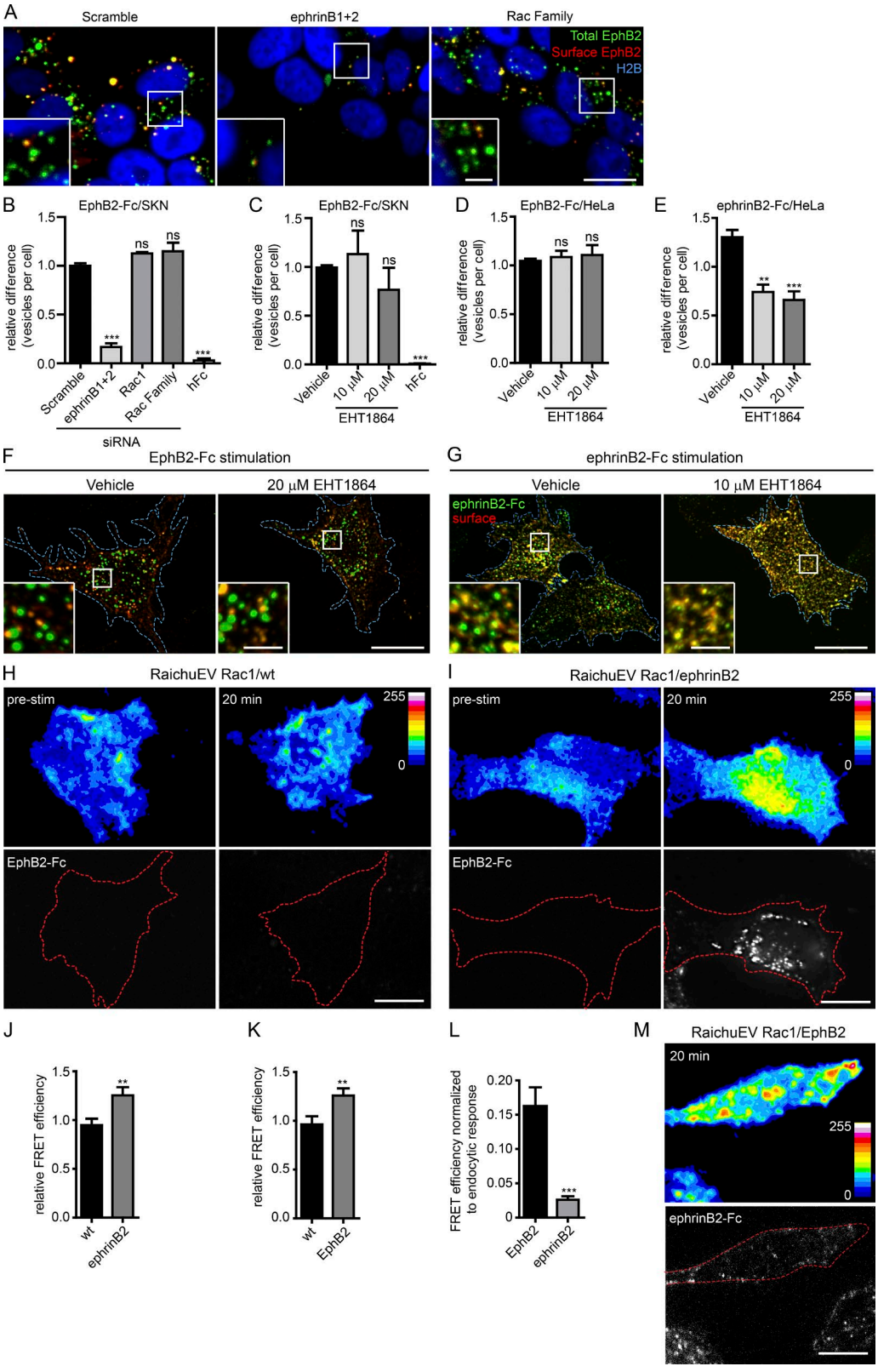

Figure 4. **Rac is not required for endocytosis of soluble EphB2-Fc.** (A) Representative images showing the effects of siRNA depletion of Rac subfamily on EphB2-Fc endocytosis in ephrinB$^+$ SKN cells. SKN cells were treated with indicated siRNAs before stimulation with fluorescently labeled, preclustered EphB2-Fc, fixed without permeabilization, and stained against Fc (surface EphB2, shown in red or yellow in the merge). Internalized vesicles appear as green puncta (total EphB2-Fc) within the vicinity of SKN nuclei (H2B channel, shown in blue). Bars: 10 µm; (inset) 2.5 µm. (B) Quantification of A, including Rac1 single depletion and hFc negative control. Images were analyzed with CellProfiler. Results are shown as mean ± SE (n = 4–6 independent experiments, >408 cells per condition per experiment, data normalized to median scramble value per experiment); ns, not significant; **, $P < 0.01$; ***, $P < 0.001$, one-way ANOVA with Dunnett's post hoc test. (C) Quantification for effect of Rac inhibitor EHT1864 versus vehicle control on EphB2-Fc

to that observed when overexpressing Tiam2ΔN in cells treated with scramble siRNA (Fig. S5 I).

In the absence of available antibodies that specifically detect endogenous Tiam2, we used the Tiam2ΔN to detect colocalization with EphB2. Indeed, immunolabeling SKN cells overexpressing Tiam2ΔN co-cultured with HeLa EphB2ΔC-mCherry donor cells revealed colocalization along filopodia contact sites, but not with internalized vesicles (Fig. 7 F). Finally, treatment of SKN cells overexpressing Tiam2ΔN with the Rac inhibitor EHT1864 before co-culture with EphB2ΔC$^+$ cells led to a robust decrease in EphB2 trans-endocytosis from 205 ± 11% to 53 ± 3% of GFP-expressing control cells (mean ± SE; Fig. 7, G and H), indicating that Rac is indeed downstream of Tiam2.

Tiam1, which has previously been implicated in both EphB and ephrinB signaling (Tanaka et al., 2004; Yoo et al., 2010; Boissier et al., 2013), was not a hit in our screen (Fig. 6 B and Table S1), a result that was confirmed in follow-up experiments with SKN cells (Fig. 6 D). Depletion of Tiam1 in HeLa cells significantly reduced EphB2 trans-endocytosis (Fig. 7, A and B). This result may be explained by the fact that Tiam1 levels are higher in SKN than HeLa cells, at least based on RT-PCR analysis (Fig. S5 J). Incomplete siRNA knockdown of Tiam1 may leave enough functional Tiam1 in SKN cells to not cause an effect, whereas the remaining levels of Tiam1 in HeLa may not be sufficient for its function. Double depletion of Tiam1 and Tiam2 did not further reduce EphB2 or ephrinB1 trans-endocytosis in HeLa cells (Fig. 7, B and C), despite efficient knockdown of Tiam1 protein (Fig. S5 F). The reason for this apparent lack of functional redundancy between Tiam1 and Tiam2 remains to be investigated. Collectively, both Tiam1 and Tiam2 are involved in regulating ephrinB–EphB trans-endocytosis, potentially in different spatiotemporal roles.

Rac activity is required for EphB2-induced cell repulsion

Finally, having established that a Rac signaling pathway regulates EphB2 trans-endocytosis, we examined how this influences the physiological response of cell repulsion after Eph–ephrin activation. To this end, we performed live imaging on SKN cells overexpressing mCherry co-cultured with donor EphB2ΔC-GFP–positive HeLa cells in the presence of either vehicle or 10 µM EHT1864 and measured the distance between two interacting cells over time after an initial point of contact. Upon cell–cell contact and trans-endocytosis, vehicle-treated SKN cells were repelled by the EphB2 donor cells (Fig. 8, A and B; and Video 5). Conversely, Rac inhibition that blocked EphB2 trans-endocytosis completely terminated the EphB2-mediated repulsion (Fig. 8, A and B; and Video 6). To ensure repulsion was specific to Eph–ephrin signaling and not simply initiated by cell–cell contact, we performed the same experiment replacing the EphB2 donor cell with a cell expressing a signaling mutant version of a nonrelated transmembrane receptor, cluster (Flrt3^{UF}-venus). Flrt3^{UF} contains a point mutation in its extracellular binding domain and thus is not able to bind its canonical targets, the Unc family (Seiradake et al., 2014). Flrt3^{UF+} HeLa cells failed to induce cell repulsion in co-cultured SKN cells (Fig. 8, A and B). We therefore conclude that cell contact–mediated repulsion requires EphB2 trans-endocytosis, which in turn is dependent on Rac activity.

Discussion

Eph–ephrin–mediated cell repulsion is essential for many developmental processes, structural plasticity in adults, regenerative conditions, and disease (Pasquale, 2008; Kania and Klein, 2016). We and others have previously shown that bidirectional trans-endocytosis of EphBs and ephrinBs promotes cell repulsion (Marston et al., 2003; Zimmer et al., 2003). Here, we have identified a conserved signaling pathway that is specifically required for trans-endocytosis of membrane-tethered EphB, but not soluble EphB2-Fc (Fig. 9). Key components of this pathway are the Rac-GEF Tiam proteins and their Rac subfamily GTPase substrates whose activities promote actin polymerization at sites of EphB2 internalization. The fact that this pathway is not required for uptake of soluble EphB2-Fc argues that the type of endocytosis activated by ephrinB reverse signaling critically depends on the biophysical properties of its "ligand," such as membrane tethering and possibly cluster size.

Endocytosis pathways in the cell are classified by distinct morphological features and target cargo and have more recently been defined by their molecular regulators. Those pathways that involve uptake of larger cargo, such as phagocytosis and macropinocytosis, form actin-structured cups that close around the target before myosin-stimulated contraction

endocytosis in ephrinB$^+$ SKN cells. Experimental design, analysis, and statistics are as described in A and B (n = 4–8 independent experiments, >345 cells per condition per experiment, data normalized to median vehicle value per experiment); statistics are as described in B. (D) Quantification of the effect of Rac inhibitor EHT1864 versus vehicle control on EphB2-Fc endocytosis in HeLa cells overexpressing ephrinB1-mCherry. Cells were stimulated with fluorescently labeled, preclustered EphB2-Fc fixed without permeabilization and immunostained against Fc (surface EphB2). Cells were imaged and manually scored for internal vesicles. Results shown as mean ± SE (n = 3–5 independent experiments, 29–128 cells per condition per experiment); statistics are as described in B. (E) Quantification of the effect of Rac inhibitor EHT1864 versus vehicle control on ephrinB2-Fc endocytosis in HeLa cells overexpressing EphB2-mCherry. Cells were stimulated with fluorescently labeled, preclustered ephrinB2-Fc or hFc, fixed, stained, and analyzed as in D (n = 3–5 independent experiments, 42–64 cells per condition per experiment, data normalized to median vehicle value per experiment); statistics are as described in B. (F and G) Representative images from D and E, respectively. Cell boundary outlined by blue border. Internalized vesicles appear as green puncta, distinct from surface signal (appears as yellow). Bars: 10 µm; (inset) 2.5 µm. (H and I) Representative images for Rac activation using RaichuEV Rac1 FRET biosensor either in wild-type (WT; H) or ephrinB2$^+$ (I) HeLa cells after stimulation with EphB2-Fc. Cells were imaged before and 20 min after fluorescently labeled, preclustered EphB2-Fc stimulation. Top panels show pseudocolor intensity code. Bottom panel shows accumulation of EphB2-Fc; the cell boundary is outlined by a dashed red border. Bars, 10 µm. (J and K) Quantification of the relative difference in Rac activation between WT and test conditions (ephrinB2$^+$ or EphB2$^+$ cells) 20 min after stimulation with either EphB2-Fc (J) or ephrinB2-Fc (K), respectively. Results are shown as mean ± SE (n = 15–19 cells per condition, data relative to prestimulation time point per each condition); **, $P < 0.01$; Student's t test. (L) Increase in Rac activity in EphB2$^+$ and ephrinB1$^+$ cells stimulated with ephrinB2-Fc or EphB2-Fc, respectively, relative to the extent of endocytosis (calculated from total fluorescent signal). Results are shown as mean ± SE (n = 15–19 cells per condition); ***, $P < 0.001$, Student's t test. (M) Representative images for Rac activation using RaichuEV Rac1 Fret biosensor in EphB2$^+$ HeLa cells after 20-min exposure to fluorescently labeled, preclustered ephrinB2-Fc. Fig. S3 B shows both prestimulation and the 20-min time point for comparison. Top panel shows pseudocolor intensity code. Bottom panel shows accumulation of ephrinB2-Fc; the cell boundary is outlined by a dashed red border. Bar, 10 µm.

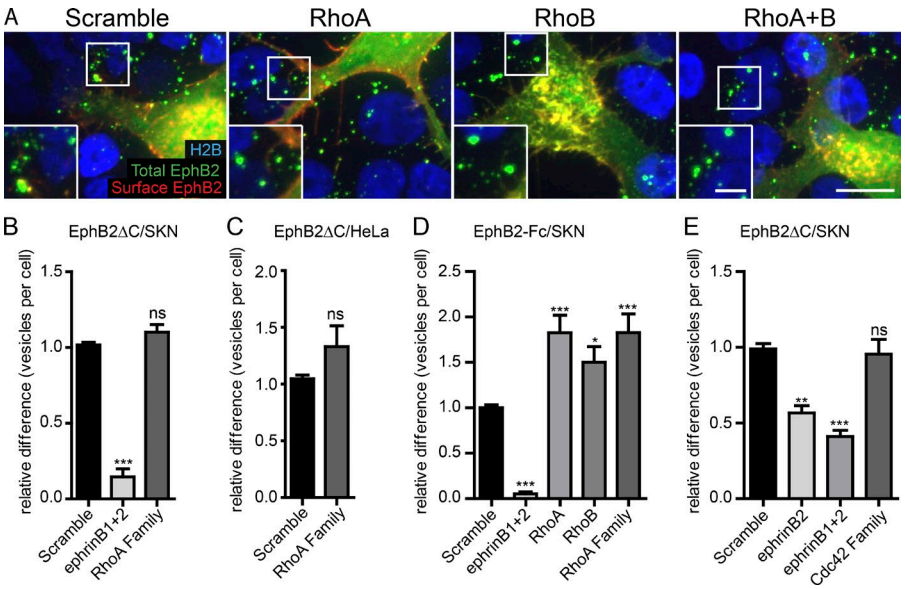

Figure 5. **The role of RhoA and Cdc42 GTPase families in EphB2ΔC trans-endocytosis.** Representative images (A) and quantification (B) showing the effect of RhoA subfamily (RhoA and RhoB) depletion on EphB2ΔC trans-endocytosis into ephrinB$^+$ SKN cells. SKN cells were treated with siRNA for 72 h before 80-min co-culture with EphB2ΔC-GFP/Flag–positive cells. Cells were fixed without permeabilization and probed against Flag (surface EphB2ΔC, shown in red or yellow in the merge). Internalized vesicles appear as green puncta (total EphB2ΔC signal) within the vicinity of SKN nuclei (H2B channel, shown in blue). Image shown as maximum projection. Bars: 10 µm; (inset) 5 µm. Acquired images were analyzed using CellProfiler. (B) Results shown as mean ± SE (n = 4 independent experiments, >120 responder cells per condition per experiment, data normalized to median scramble value per experiment); ns, not significant; *, P < 0.05; **, P < 0.01; ***, P < 0.001, repeated measures one-way ANOVA with Dunnett's post hoc test. (C) Quantification for the effect of RhoA subfamily depletion on EphB2ΔC trans-endocytosis into HeLa cells. HeLa cells overexpressing ephrinB1-mCherry were treated with siRNA for 48 h before 80 min co-culture with EphB2ΔC-GFP/Flag$^+$ cells. Cells were fixed without permeabilization and probed against Flag (surface EphB2ΔC). Cells were manually scored for internal vesicles. Results shown as mean ± SE, n = 3 independent experiments, 19–36 responder cells per condition per experiment, statistics as in B. (D) Quantification showing the effect of RhoA subfamily depletion on EphB2-Fc endocytosis in ephrinB$^+$ SKN cells, representative images shown in Fig. S4B. SKN cells were treated with indicated siRNAs before stimulation with fluorescently labeled, preclustered EphB2-Fc, fixed without permeabilization and stained against Fc (surface EphB2). Images were analyzed with CellProfiler™. Results shown as mean ± SE, n = 3 independent experiments, >463 cells per condition per experiment, data normalized to median scramble value per experiment; statistics as in B. (E) Quantification showing the effect of Cdc42 subfamily depletion on EphB2ΔC trans-endocytosis into ephrinB$^+$ SKN cells. Experimental design and analysis as described in A and B (n = 3 independent experiments, >232 cells per condition per experiment, data normalized to median scramble value per experiment). *, P < 0.05; **, P < 0.01; ***, P < 0.001, one-way ANOVA with Dunnett's post hoc test.

promotes internalization (Swanson, 2008). Where Eph–ephrin trans-endocytosis differs, is in the unique requirement of physically pinching off parts of the opposing cell membrane as compared with engulfing the entire "prey"–receptor complex. Actin polymerization was previously shown to associate with internalization into EphB$^+$ cells, but surprisingly not ephrinB$^+$ cells (Marston et al., 2003). Using live imaging to track actin polymerization and EphB2 uptake into ephrinB$^+$ cells, we show here that polymerized actin in fact colocalizes with sites of EphB2 internalization. Moreover, this response is dependent on Rac activity, similarly to what has been described for ephrinB trans-endocytosis. Beyond the role of actin and Rac, little is known on the physical processes underlying Eph–ephrin internalization and the morphological features of trans-endocytosed vesicles.

The requirement of Rac-stimulated actin polymerization at the site of Eph–ephrin–mediated cell contact may appear paradoxical considering that traditional roles of Eph–ephrin signaling comprise cell retraction and growth cone collapse, which require depolymerization of actin. In EphB2-Fc–stimulated hippocampal neuron cultures, previous work showed that neurite retraction was driven by RhoA (and not Rac) and its effector kinase, ROCK (Takeuchi et al., 2015). Conversely, in a cell–cell context, membrane-bound EphB2 stimulated neurite retraction in a Rac-dependent manner (Xu and Henkemeyer, 2009). In the case of ephrinA1-induced EphA4 growth cone collapse, phosphorylation of the GEF ephexin leads to increased specificity for RhoA compared with Rac1 and Cdc42 (Shamah et al., 2001). Moreover, a Rac-to-Rho switch has been seen for other signaling systems. Initial endocytosis of the signaling molecule NogoA was shown to require Rac activation, followed by a change to RhoA-mediated signaling during its retrograde transport to the cell body, inducing growth-cone collapse (Joset et al., 2010). Here, we observed a loss of colocalization between high levels of F-actin as the vesicle trafficked internally, in line with a possible switch from Rac to Rho activity. It would be important in the future to see if Rho is indeed activated after Rac-induced internalization occurs and to determine the factors that cause the change.

In analyzing the requirement of Rac for EphB2 trans-endocytosis, we discovered a high degree of redundancy among Rac subfamily members Rac1, Rac3, and RhoG. Although we saw no effect when depleting one family member or two subfamily members simultaneously, a significant reduction was seen when targeting all three GTPases. The ubiquitously expressed Rac1 and neuron-specific Rac3 have previously been shown to act together in nervous system development (Corbetta et al., 2009), whereas RhoG is thought to act either upstream or in parallel to Rac and Cdc42 (Wennerberg et al., 2002; Dyer et al., 2010; Franke et al., 2012). As with Rac1, RhoG plays an important role in phagocytosis of large cargo (Nakaya et al., 2006). Moreover, there is cross talk between GEFs that regulate Rac and those for RhoG. In agreement with our findings, and what has previously been shown for Eph–ephrin signaling, the Vav GEFs target both Rac1 and RhoG (Jaiswal et al., 2013), thus providing a branching point from ephrin activation. This suggests redundancy at the level of not only GTPases but also GEFs, and it may explain the only modest, yet significant, reduction we observe when knocking down Rac subfamily GTPases or Rac-GEFs, compared with ephrinB itself. An alternative explanation for the modest effects may be reduced knockdown efficiency when targeting multiple proteins. Indeed Western blotting revealed weakened knockdown efficiency in the triple depletion, in particular for Rac1, compared with single depletions.

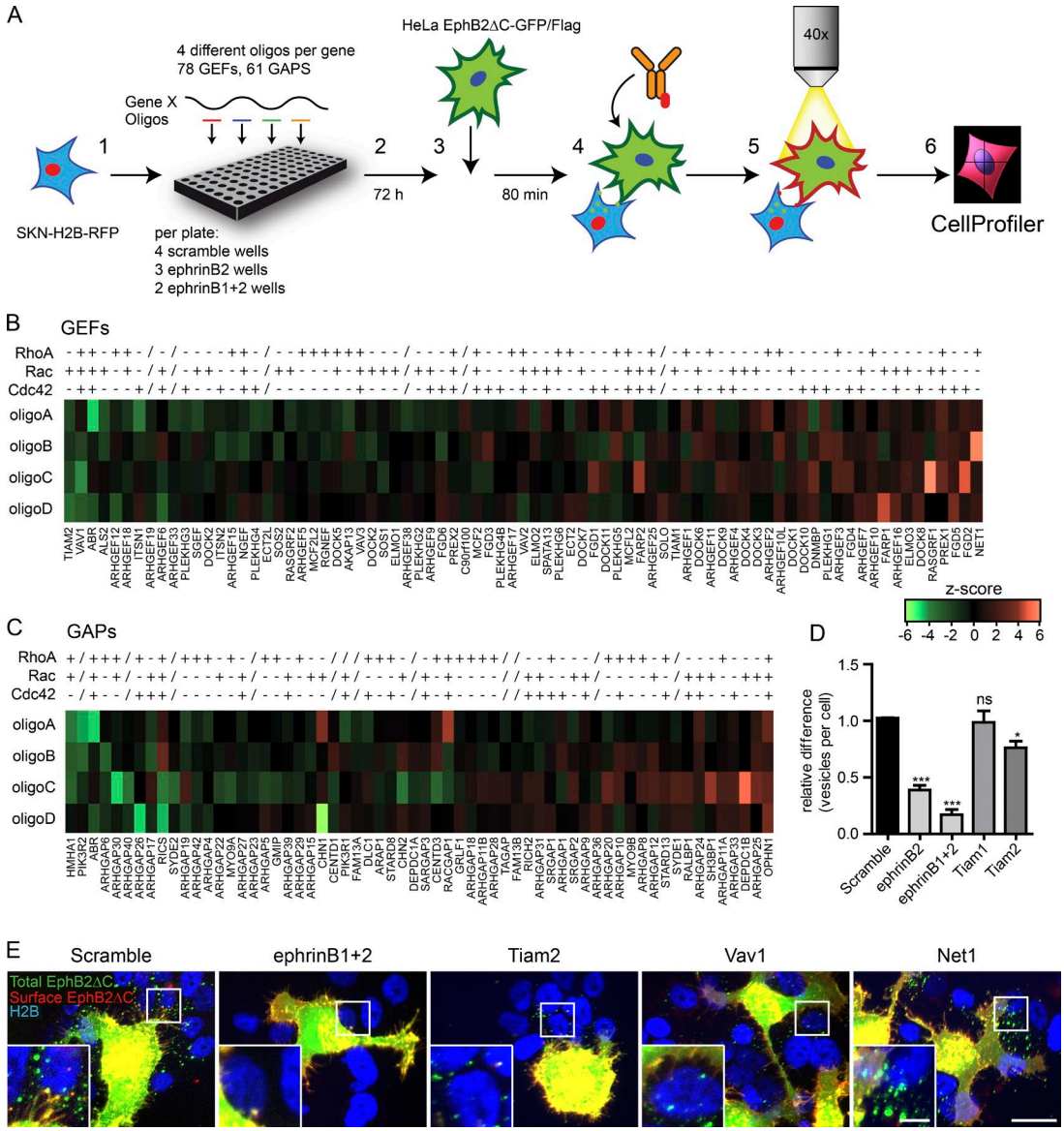

Figure 6. **Functional siRNA screen for Rho family GEFs and GAPs.** (A) Basic screen design: (1) ephrinB$^+$ SKN-H2B-RFP cells were seeded into 96-well imaging plates and library of siRNA oligos were added. (2) Cells were incubated for 72 h and (3) co-cultured for 80 min with HeLa EphB2ΔC-GFP/Flag cells prestained with CellTracker green. (4) Cells were then fixed without permeabilization and immunostained against Flag. (5) Cells were imaged, and (6) semiautomated data analysis was performed using CellProfiler. On average, 150 responder cells per well were analyzed. (B and C) Heatmap for mean z-score values of the two independent runs showing all four siRNA oligos (A–D) per gene for all GEFs or GAPs, respectively. Specific GEF or GAP activity for each GTPase subfamily is indicated, taken from previous studies (Tcherkezian and Lamarche-Vane, 2007; Jaiswal et al., 2013; Cook et al., 2014) and independent literature search (+, active toward at least one member of subfamily; –, negative for all members of subfamily; /, unknown specificity). Genes are ranked from mean z-score of all four siRNA oligos. Values shown by intensity profile. (D) Quantification showing the requirement of Tiam2 for EphB2ΔC trans-endocytosis into ephrinB$^+$ SKN cells. Experiment design and analysis as described in A. Results shown as mean ± SE, (n = 5 independent experiments, 44–449 responder cells per condition per experiment). ns, not significant; *, P < 0.05; **, P < 0.01; ***, P < 0.001, repeated measures one-way ANOVA with Dunnett's post hoc test. (E) Example images of scramble siRNA controls and top-ranked hits. Total EphB2ΔC is shown in green, surface EphB2ΔC in red, and SKN-H2B in blue. Bars: 20 µm; (inset) 2.5 µm.

We induced a more robust response when treating the cells with the pan-Rac inhibitor EHT1864. EHT1864 is known to target Rac1, 2, and 3 (Shutes et al., 2007), but it is not known whether it blocks RhoG activity. As EHT1864 treatment did not reduce EphB2 trans-endocytosis to the extent of double depleting ephrinB1 and 2 in SKN cells, it is possible that the remaining uptake occurs via RhoG. Alternatively, Cdc42 and its subfamily members could also play a secondary role, and therefore, we did not see a complete block. Importantly, we confirmed the requirement of Rac for EphB2 trans-endocytosis using EHT1864 in multiple cell types, including SKN cells that endogenously express ephrins, HeLa cells overexpressing ephrins, and primary cultured mouse cortical neurons. Furthermore, although most experiments have been conducted with an EphB2ΔC construct to solely focus on trans-endocytosis into the ephrinB$^+$ cell, trans-endocytosis using donor cells expressing full-length EphB2 instead was equally sensitive to Rac inhibition. This underlines that the truncated EphB2 is functionally equivalent to its full-length counterpart in inducing reverse trans-endocytosis.

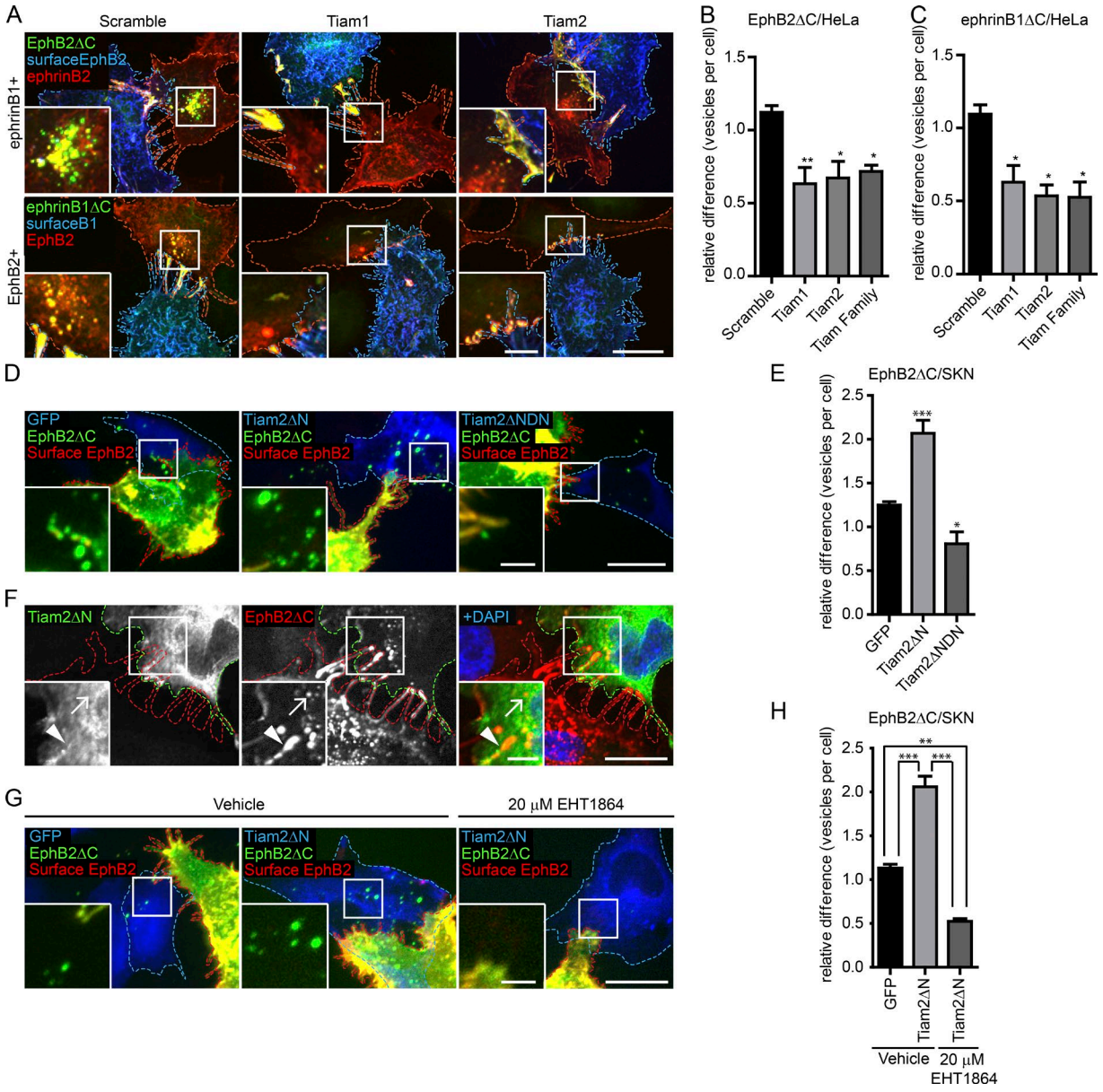

Figure 7. **Tiam2 mediates EphB2 and ephrinB1 trans-endocytosis.** Representative images (A) and quantification (B and C) showing the requirement of Tiam1 and Tiam2 for EphB2ΔC and ephrinB1ΔC trans-endocytosis into HeLa cells expressing either ephrinB1 (A and B, top row) or EphB2 (A and C, bottom row), respectively. HeLa responder cells were treated with Tiam1/2 siRNAs, alone or in combination 48 h before 80-min co-culture with donor cells. The donor cell boundary is outlined by a dashed blue border, and the responder cell boundary is outlined by a dashed red border. Internalized vesicles appear as green puncta, distinct from surface signal (appears as yellow). Number of internalized vesicles per cell was counted manually as described in Fig. 2 F. Bars: 10 µm; (inset) 2.5 µm. (B and C). Results shown as mean ± SE (n = 3–4 independent experiments, 9–57 responder cells per condition per experiment, data normalized to median scramble value per experiment). *, P < 0.05; **, P < 0.01; ***, P < 0.001, one-way ANOVA with Dunnett's post hoc test. Representative images (D) and quantification (E) for the effect of overexpressing Tiam2 constructs on EphB2ΔC trans-endocytosis into ephrinB$^+$ SKN cells. SKN responder cells (blue dashed outline) overexpressing GFP (left, pseudocolored blue), Tiam2ΔN-GFP/HA (Tiam2ΔN, center, pseudocolored blue), or dominant-negative Tiam2ΔN-GFP/HA (Tiam2ΔNDN, right image, pseudocolored blue) were co-cultured with EphB2ΔC-mCherry/Flag–positive cells (red dashed outline, pseudocolored green). Cells were fixed without permeabilization and probed against Flag (surface EphB2ΔC, shown in yellow). Internalized vesicles appear as green puncta in the SKN cells. Images are shown as maximum projection. Bars: 20 µm; (inset) 5 µm. (E) Results shown as mean ± SE (n = 4 independent experiments, 26–88 responder cells per condition per experiment, data normalized to median of GFP control condition); statistics as in Fig. 2C. (F) Tiam2 colocalization with EphB2 at contact sites. HeLa responder cells (green outline) overexpressing Tiam2ΔN-GFP/HA (shown in green in the merge) and untagged ephrinB2 were co-cultured with Hela donor cells (red outline) overexpressing EphB2ΔC-mCherry (red in the merge). Cells were fixed on ice, permeabilized, and immunostained against HA and DAPI. Arrowhead indicates contact site, and arrow indicates internalized vesicle. Bars: 10 µm; (inset) 2.5 µm. Representative images (G) and quantification (H) for the effect of Rac inhibitor EHT1864 versus vehicle control on EphB2ΔC trans-endocytosis into ephrinB$^+$ SKN cells overexpressing Tiam2. SKN responder cells (blue dashed outline) overexpressing GFP (left, pseudocolored blue) or Tiam2ΔN-GFP/HA (Tiam2ΔN, middle and right, pseudocolored blue) were treated for 4 h with either vehicle (left and middle) or 20 µM EHT1864 (right) before co-culture withEphB2ΔC-mCherry/Flag$^+$ cells (red dashed outline, pseudocolored green). Cells were fixed without permeabilization and probed against Flag (surface EphB2ΔC, shown in yellow). Internalized vesicles appear as green puncta in the SKN cells. Images are shown as maximum projection. Bar, 20 µm, inset Bar, 5 µm. (H) Results shown as mean ± SE (n = 3 independent experiments, 26–60 responder cells per condition per experiment, data normalized to median of vehicle-treated/GFP-expressing control condition). **, P < 0.01; ***, P < 0.001, one-way ANOVA with Bonferroni post hoc test.

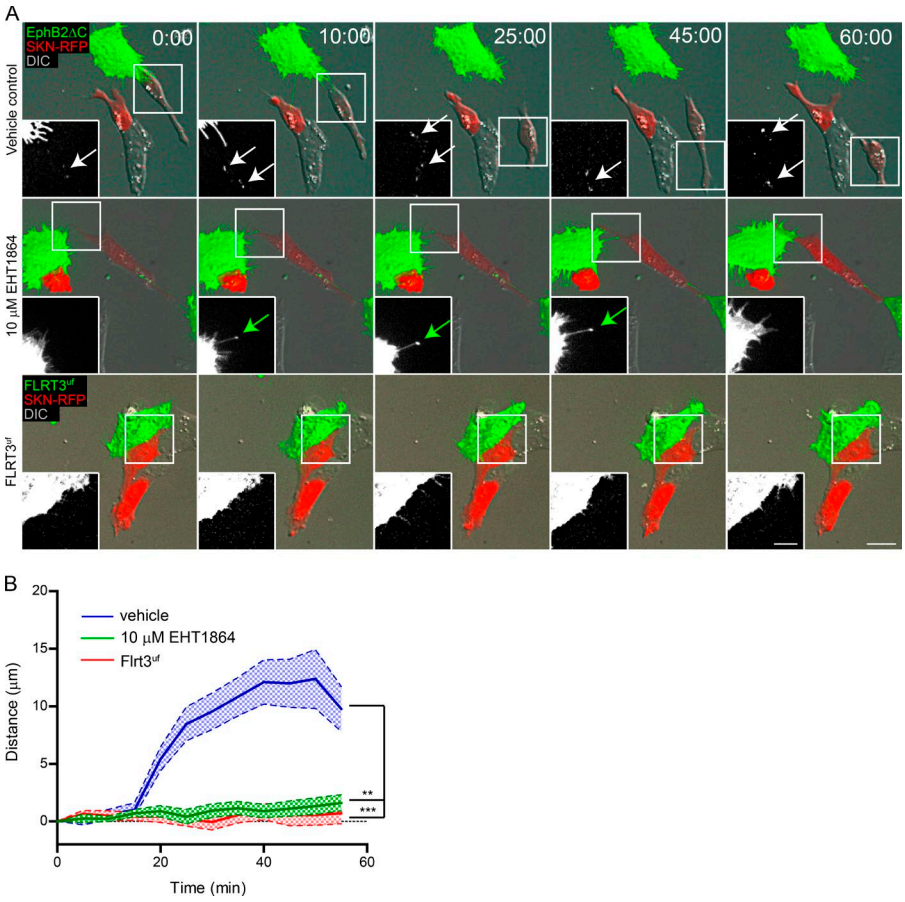

Figure 8. **Rac mediates EphB2-triggered cell repulsion.** Time-lapse images (A) and quantification (B) of the effect of Rac inhibitor EHT1864 and the requirement of EphB2 for cell repulsion in ephrinB$^+$ SKN cells expressing mCherry (red). SKN cells were treated for 4 h with either vehicle or 10 µM EHT1864 before co-culture with cells expressing either EphB2ΔC-GFP (shown in green, top and middle rows) or FLRT3^{UF}-Venus (shown in green, bottom row). Cells were imaged every 5 min. Inserts show the green channel, white arrows denote internalized vesicles, and green arrows indicate contact site without internalization. Maximum projection of deconvolved images. Bars: 25 µm; (inset) 12.5 µm. Elapsed time shown as minutes :seconds. (B) Measured distance between donor and responder cells over time for each condition shown as mean ± SE (n = 25–50 cells from three independent experiments); **, $P < 0.01$; ***, $P < 0.001$, two-way ANOVA.

Activation of EphB–ephrinB signaling ultimately leads to cell retraction and repulsion. Neurite retraction for primary cultures of ephrinB3-expressing mouse hippocampal neurons and immortalized neuronal cell lines, both stimulated by co-culture with EphB2$^+$ cells, has been shown to be Rac dependent (Xu and Henkemeyer, 2009). Moreover, the activated ephrinB3 recruits the adaptor protein Grb4, which in turn tethers Dock1, activating both Rac1 and Cdc42, as well as their downstream target Pak to instigate neurite retraction/pruning. In accordance with this, here we show a correlation between EphB2 trans-endocytosis and cell–cell-mediated repulsion in ephrinB$^+$ cells, with both processes being reliant on Rac activity.

Although EphB trans-endocytosis of membrane-tethered EphB from an opposing cell into the ephrinB$^+$ cell requires Rac activity, uptake of soluble EphB ectodomain into the ephrinB$^+$ cell does not. Surprisingly, this was specific for the endocytic machinery activated by ephrinB reverse signaling, as endocytosis of ephrinB2-Fc into EphB2$^+$ cells was reliant on Rac activity. What could be the reason for this differential effect? Using a Rac-activity specific biosensor, we showed that soluble stimulation of both ephrinB and EphB activated Rac. However, the degree of Rac activity in ephrinB-Fc–stimulated EphB2 cells was far greater than that in EphB2-Fc–stimulated ephrinB1 cells when considering the difference in abundance of protein uptake. These results raise several important points. First, different mechanisms are used for soluble EphB2 uptake and membrane-bound trans-endocytosis. Clathrin-mediated endocytosis (CME) has been suggested as a means of soluble EphB endocytosis into ephrinB$^+$ cells (Parker et al., 2004); however, co-culture experiments indicated CME to not be involved in trans-endocytosis, albeit for ephrinB into EphB$^+$ cells (Marston et al., 2003; Zimmer et al., 2003). Nevertheless, this supports the idea of a different mechanism between the soluble and membrane-tethered uptake and highlights the importance of using a cell–cell assay when describing the machinery for Eph–ephrin–mediated cell repulsion. Second, at the level of signaling pathways activated, multiple differences were previously found between soluble, cell–cell, and ephrinB-stimulated or EphB-stimulated cells (Jørgensen et al., 2009), despite the final cellular response (retraction) being the same. It is therefore not surprising that differences also exist at the level of endocytic regulation. It remains to be shown if Rac activity differs between EphB and ephrinB trans-endocytosis. Unfortunately, limitations in fluorophore overlap meant we could not use the Rac biosensor in a cell–cell assay, and GTP-loaded Rac pull-down assays are not sensitive enough given the spatiotemporal resolution required. Remarkably, a recent study in our group has revealed that Eph receptors and ephrins are released in signaling-competent exosomes (Gong et al., 2016), and it will be interesting to determine which of the two modes of endocytosis is used for their uptake.

The role of RhoA in Eph–ephrin signaling has previously been associated with cell collapse without mention of endocytosis (Sahin et al., 2005; Groeger and Nobes, 2007; Takeuchi et al., 2015). Indeed, here we saw no effect on trans-endocytosis after depletion of either RhoA or RhoB or both together. Depletion of RhoA subfamily members did, however, increase the number of EphB2-Fc vesicles in ephrinB$^+$ cells. RhoA has been shown to be a negative regulator of CME (Kaneko et al., 2005; Khelfaoui et al., 2009), and if soluble EphB2-Fc uptake occurs

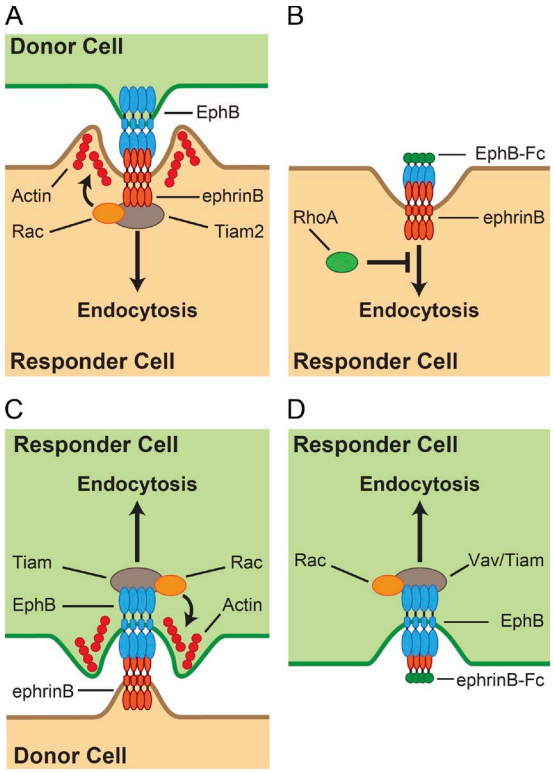

Figure 9. **Models for the regulation of EphB–ephrinB endocytosis.** (A) EphB2 trans-endocytosis into ephrinB$^+$ cells requires Tiam2, activating Rac subfamily GTPases leading to actin cytoskeleton rearrangement and ligand–receptor internalization. Direct interaction between ephrinBs and Tiam2 has previously been established (Terawaki et al., 2010). (B) EphB2-Fc soluble uptake into ephrinB$^+$ cells does not require Rac or Tiam but is negatively regulated by RhoA subfamily GTPases. (C) EphrinB trans-endocytosis into EphB2$^+$ cells uses a similar mechanism to EphB2 trans-endocytosis. (D) EphrinB2-Fc uptake into EphB2$^+$ cells is dependent on both Tiam and Vav family GEFs and Rac activity (Tanaka et al., 2004; Cowan et al., 2005; Tolias et al., 2007).

via this pathway, depletion of RhoA may relieve this block. Cdc42 has been implicated in EphB2 signaling via its GEF, intersectin. EphB2/intersectin activity led to Cdc42-driven actin polymerization regulating hippocampal spine maturation (Irie and Yamaguchi, 2002; Nishimura et al., 2006). Here, we saw no effect on EphB2 trans-endocytosis; however, we cannot rule out redundancy with the Rac subfamily of GTPases masking the response. Ultimately, we found neither RhoA nor Cdc42 subfamilies to be of great influence on EphB2 trans-endocytosis, whereas the Rac subfamily appears to play a leading role.

To understand the regulation of GTPases in EphB2 trans-endocytosis, we performed an siRNA screen against Rho family GEFs and GAPs. Although using the literature to categorize specificity for each GEF and GAP to a GTPase is to a degree ambiguous, in general, data from our screen showed a trend for positive regulation of EphB uptake by Rac GEFs, i.e., their knockdown resulted in a decrease of EphB2 trans-endocytosis, with our strongest hits being Tiam2 and Vav1. This result is reminiscent of previous studies that implicated other members of both subfamilies (Tiam1 and Vav2/Vav3, respectively) in Eph–ephrin internalization and signaling, although no study linked these GEFs to contact-mediated trans-endocytosis (Tanaka et al., 2004; Cowan et al., 2005; Tolias et al., 2007; Um et al., 2014). The fact that Tiam2 depletion reduced, and overexpression of a constitutively active Tiam2 construct increased EphB2 trans-endocytosis suggests that the GEF is the rate-limiting factor in this endocytic machinery. In support of Tiam2 being upstream of Rac activation, the increase in EphB2 trans-endocytosis was completely blocked upon Rac inhibition. Finally, Tiam2 colocalized with the EphB2–ephrinB clusters at contact sites, which functionally supports structural data that mapped binding of Tiam2 on ephrinB (Terawaki et al., 2010). This specific spatiotemporal colocalization would restrict Rac activation at sites of contact, thus promoting localized F-actin formation to drive trans-endocytosis.

Although Tiam2 has never been implicated in Eph–ephrin endocytosis or signaling, Tiam1 has been shown to regulate Eph forward and ephrinB reverse signaling in different contexts after stimulation with Eph-Fc or ephrin-Fc fusion proteins (Tanaka et al., 2004; Tolias et al., 2007; Um et al., 2014). Considering previous and present results, it seems likely that Tiam1 and 2 play similar roles in regulating EphB2 trans-endocytosis and further act as Rac activators in Eph–ephrin signaling. Vav2 has previously been shown to be required for ephrinB-Fc endocytosis (Cowan et al., 2005), but neither Vav2 nor Vav3 knockdown induced a strong effect in our co-culture screen. It remains to be investigated if this is caused by functional redundancy between the Vav proteins (Cowan et al., 2005) or the assay that was used. Another interesting hit that reduced EphB trans-endocytosis was Abr, a protein that antagonizes Tiam1-stimulated Rac activity downstream ephrinB-induced EphB2 forward signaling (Um et al., 2014). Why Abr depletion reduced rather than promoted EphB2 trans-endocytosis in our screen remains to be investigated. In contrast to the GEFs that positively regulate EphB2 trans-endocytosis, no specific pattern for a preferred GTPase was seen for the four GEFs that negatively regulated EphB2 uptake. Only Fgd2 has been previously linked to endocytosis, where it regulated Cdc42-dependent membrane ruffles and colocalizes with early endosomes (Huber et al., 2008).

Fittingly, the three GAPs whose depletion led to the opposite response, namely an increase in EphB2 trans-endocytosis (Ophn1, Arhgap25, and Depdc1b), all have been linked to Rac activity. Interestingly, Ophn1, which shows activity toward Rac and RhoA, is an X-linked mental retardation protein involved in synaptic vesicle endocytosis (Nakano-Kobayashi et al., 2009). Arhgap25, which shows specificity toward Rac, acts as a negative regulator of phagocytosis (Csépányi-Kömi et al., 2012), whereas work on Depdc1b has focused on its role in mitotic progression (Marchesi et al., 2014). Four of the five GAPs whose depletion decreased EphB2 trans-endocytosis, i.e., that positively regulated trans-endocytosis, target RhoA, although most not exclusively, and none of them have been linked to the endocytic machinery. Taking all our results together, we saw a trend for positive regulation of EphB2 trans-endocytosis through Rac and negative regulation of EphB2-Fc uptake through RhoA. Moreover, we detected some promising targets already linked to Eph–ephrin signaling or endocytosis, and we discovered possible novel functions for Rho GEFs and GAPs that have not been studied extensively or only studied in other unrelated cellular contexts.

Collectively, our data demonstrate that ephrinB$^+$ cells use a conserved signaling pathway to endocytose EphB2 from opposing cells and thereby enable contact-mediated repulsion. This pathway may be relevant not only for the development and physiology of neuronal circuits and other organ systems but also for pathological situations. EphrinB2 serves as the entry

receptor for paramyxovirus Nipah virus (Negrete et al., 2005), and recent work suggests that NiV entry occurs by an endocytic mechanism (Pernet et al., 2009). Moreover, Eph–ephrin signaling is heavily implicated in cancer pathogenesis, including invasiveness and metastatic potential (Pasquale, 2010), raising the possibility that migrating cancer cells use trans-endocytosis for efficient cell detachment.

Materials and methods

Cell culture, transfection, and inhibitor treatment

SKN cells and SKN cells stably expressing Histone2B-dual-RFP (SKN H2B-RFP) were cultured in Opti-MEM with Glutamax (Thermo Fisher Scientific). HeLa and Hek293 cells were cultured in DMEM (Thermo Fisher Scientific). All cell media were supplemented with 10% fetal calf serum (GE Healthcare) and 1% penicillin/streptomycin (Thermo Fisher Scientific). Medium for HeLa cells stably expressing EphB2ΔC-GFP/Flag was supplemented with 1% Geneticin (Thermo Fisher Scientific).

Primary dissociated cultures of cortical neurons were generated from embryonic day 15.5 embryos of wild-type CD1 mice. Neurons were cultured in 8-well imaging chambers (Ibidi) coated with 1 mg/ml Poly-D-lysin and 5 µg/ml laminin in Neurobasal medium supplemented with 2% B27 supplement (Thermo Fisher Scientific), 10 mM glutamine (GE Healthcare), and 1% penicillin/streptomycin (Thermo Fisher Scientific) and incubated at 37°C and 5% CO_2.

Cell lines were transfected using Lipofectamine 2000 reagent (Thermo Fisher Scientific) according to the manufacturer's instructions. Constructs used were EphB2-mCherry, EphB2FL-GFP/Flag, EphB2ΔC-GFP/Flag, untagged EphB2ΔC, ephrinB1-mCherry, ephrinB1ΔC-GFP/HA, untagged ephrinB2ΔC (all adapted from Zimmer et al., 2003), LifeAct-mCherry-N1 (plasmid 40908; Addgene; Smyth et al., 2012), RaichuEL Rac1 (gift from T. Biederer, Yale University, New Haven, CT), RhoQ-GFP (plasmid 23232; Addgene; Roberts et al., 2008), RhoU-Myc/Flag (PS100001; OriGene), mouse Tiam2ΔN-GFP/HA, Tiam2ΔNDN-GFP/HA (gift of A. Malliri, Cancer Research UK, Manchester, England, UK), FLRT3^{UF} (Seiradake et al., 2014), mCherry, and GFP empty vectors. An siRNA-resistant version of Rac1 (Rac1^{r}) was generated by introducing two silent mutations to the leucine in position 4 (CTG→TTA) of wild-type Rac1, the siRNA target site. SKN-H2B-RFP cells were generated using Histone2B-dual-RFP (gift of M. Bickle, Max Planck Institute of Molecular Cell Biology and Genetics, Dresden, Germany).

Cells were transfected with siRNA oligos using Lipofectamine RNAiMax (Thermo Fisher Scientific) transfection reagent according to the manufacturer's instructions. Unless otherwise stated, cells were reverse transfected at seeding. Cells were incubated for either 72 h (SKN cells) or 48 h (HeLa cells) at 37°C. Stealth siRNA oligonucleotides were purchased from Thermo Fisher Scientific. Oligonucleotides used were ephrinB1 5′-GAAGGGCUUGGUGAUCUAUCCGAAA-3′, ephrinB2 5′-ACUAUACCCACAGAUAGGAGACAAA-3′, Rac1 5′-CCGGUGAAUCUGGGCUUAUGGGAUA-3′, Rac3 5′-CCUCCGCGACGACAAGGACACCAUU-3′, RhoG 5′-CAGGAGGAGUAUGACCGCCUCCGUA-3′, RhoA 5′-GCCUGUGGAAAGACAUGCUUGCUCA-3′, RhoB 5′-ACACCGACGUCAUUCUCAUGUGCUU-3′, Cdc42 5′-CACAACAAACAAAUUUCCAUCGGAA-3′, RhoQ 5′-AAUGACCGAUGUCUUCCUUAUAU-3′, RhoU 5′-CCUCAUUGAGUUGGACAAAUGCAAA-3′, Tiam1 5′-CAGCACAACCCUGACUGCGACAUUU-3′, and Tiam2 5′-GGGAGAACUUCAGGCGUCACAUAAA-3′. Sequences for Stealth siRNA oligonucleotides used in the trans-endocytosis screen can be found in Table S1.

Rac inhibitor EHT1864 (Tocris Bioscience) was diluted in H_2O, and cells were incubated with EHT1864 for 4 h at 37°C at the specified concentrations. As a control, cells were treated with the equivalent volume of H_2O in parallel. Cell viability in the presence EHT1864 was determined using a 3-(4,5-dumethylthiazol2-yl)-2,5-diphenyltetrazolium bromide reducing assay as described previously (Gaitanos et al., 2004).

RT-PCR

RNA was isolated from serum-starved SKN and HeLa cells using RNeasy extraction kit (QIAGEN). RT-PCR was performed using One-Step RT-PCR kit as per the manufacturer's instructions (QIAGEN).

Antibodies

The following primary antibodies were used: α-tubulin (1:5,000; 9E10; Sigma-Aldrich), Flag (1:1,000; F7425; Sigma-Aldrich), RhoG (1:500; SAB4501718; Sigma-Aldrich), RhoA (1:1,000; 26C4; Sigma-Aldrich), RhoB (1:1,000; 119; Sigma-Aldrich), Rac1 (1:1,000; ab33186; Abcam), Rac3 (1:1,000; ab124943; Abcam), Cdc42 (1:500; ab41429; Abcam), HA (1:1,000; 3F10; Roche), GFP (1:1,000; Takara Bio Inc.), Tiam1 (1:500; C-16; Santa Cruz Biotechnology, Inc.), and Tiam2 (1:1,000; P17; Santa Cruz Biotechnology, Inc.). All secondary antibodies were purchased from Jackson ImmunoResearch Laboratories, Inc. HRP-coupled secondary antibodies were used for Western blots, and fluorescently labeled secondary antibodies were used for immunostaining.

Western blots

Cell lysates were prepared using a standard protocol in Tris lysis buffer (50 mM Tris, pH 7.4, 150 mM NaCl, 2 mM EDTA, 1% Triton-X 100, and protease and phosphatase inhibitor cocktails as per the manufacturer's instructions [Roche]). Samples were loaded on SDS-PAGE gels for separation and transferred onto a polyvinylidene fluoride membrane (Merck) using a semidry blot chamber (Trans-blot SD; Bio-Rad Laboratories). Membranes were blocked using 5% skim milk in TBS with 0.1% Tween-20. Proteins of interest were probed with primary antibodies followed by HRP-coupled secondary antibodies. Antibodies were detected with either ECL Western blot reagent (GE Healthcare) or SuperSignal Femto Maximum Sensitivity Substrate (Thermo Fisher Scientific) in a Fusion FX7 chemiluminescence imaging chamber (PeqLab GmbH) with a binning of 2. Rac activity pull-down was performed using a commercially available kit according to the manufacturer's instructions (Cytoskeleton, Inc.).

Trans-endocytosis assay

SKN-H2B-RFP cells were seeded in a black, 96-well, flat-bottom glass imaging plate (Greiner Bio One GmbH) while FL-EphB2-mCherry–positive or FL-ephrinB1-mCherry–positive HeLa cells were cultured on coverslips. Cells were treated as stated in the text and serum-starved in Opti-MEM overnight before stimulation. HeLa cells stably expressing EphB2ΔC-GFP/Flag or transiently transfected with EphB2ΔC-GFP/Flag, EphB2FL-GFP/Flag, or ephrinB1ΔC-GFP/HA were used as donor cells. Donor cells were harvested with 0.02% EDTA in PBS without magnesium and calcium (Thermo Fisher Scientific) and co-cultured with responder cells for 80 min at 37°C. Cells were fixed with ice cold 4% PFA/4% sucrose. Cells were blocked in 3% BSA, and surface clusters were immunostained with anti-Flag antibody and fluorescently coupled secondary antibody. Additional permeabilization with 0.1% Triton-X 100 in PBS for 5 min was used for DAPI staining. For colocalization with Tiam2, cells were permeabilized after fixation and no surface staining was performed.

For LifeAct trans-endocytosis assay, wild-type SKN cells transiently expressing LifeAct-mCherry were seeded in a 3-mm glass-bottom imaging culture dish (MatTek Corporation). Cells were treated

with vehicle or EHT1864 4 h before stimulation with EphB2ΔC-GFP–positive HeLa donor cells. Donor cells were harvested with 0.02% EDTA in PBS without magnesium and calcium (Thermo Fisher Scientific) and seeded on to SKN cells. Cells were live-imaged every 90 s using z-stack every 0.5 µm. Nearest-neighbors 2D deconvolution and maximum projection was performed using MetaMorph software (Molecular Devices). Colocalization was determined measuring fluorescence intensity in both channels using Fiji (Schindelin et al., 2012).

Trans-endocytosis assay with primary cortical neurons

Neurons were stained with 1 µM CellTracker green (Thermo Fisher Scientific) and incubated with EHT1864 or vehicle control at the specified concentrations at 37°C and 5% CO_2 for 4 h before EphB2ΔC-mCherry–positive HeLa coseeding and live image acquisition. A single confocal plane was taken at each position at 3-min intervals for a total duration of 3 h. Images were analyzed with MetaMorph. Contact points between neurons and EphB2ΔC-mCherry–positive HeLa cells were tracked and scored for internalization.

Endocytosis assay with soluble Eph or ephrin ectodomains

The assay was adapted from Zimmer et al. (2003). Responder cells were seeded and treated as in the trans-endocytosis assay. Human IgG-Fc alone (hFc; control) or fused to ectodomains of either EphB2 or ephrinB2 (R&D Systems) were preclustered with dylight488-coupled α-humanFc antibodies in volume ratio 5:1 for 45 min at room temperature. Cells were incubated with the clustered proteins at a final concentration of 2 µg/ml for 30 min at 37°C. Incubation time was reduced to 2 min and an extra 3 min on ice to prevent internalization when determining surface expression of ephrins. Cells were fixed on ice with 4% PFA/4% sucrose. Staining for surface clusters was performed with dyLight649 α-humanFc antibodies. HeLa cells were additionally permeabilized with 0.1% Triton X-100 for 5 min and stained with DAPI.

Image acquisition and processing

Imaging was performed on an Axioobserver Z1 inverted microscope (ZEISS) equipped with a CSU-X1 spinning disc confocal unit (Yokogawa Electric Corporation) controlled by VisiView software (Visitron Systems) and a CoolSnapHQ^2 CCD camera (Photometrics). For live imaging, a temperature-controlled CO_2 incubation chamber (Pecon GmbH) was used at 37°C and 5% CO_2. Excitation was provided by lasers of 405, 488, 561, or 640 nm wavelength (Visitron Systems). 96-well plate, neuron trans-endocytosis, and cell repulsion experiments were imaged using a 40× 0.95 NA Plan-Achromat air objective (ZEISS). In 96-well plates, multiple positions were selected per well, and z-stacks of eight planes with 1 µm step size were acquired. HeLa cells on coverslips were imaged with a Plan-Achromat 63× 1.4 NA oil-immersion objective or an α-Plan 100× 1.45 NA oil-immersion objective (ZEISS). Z-stacks of 15 planes of 0.5 µm step size were acquired. Live imaging of trans-endocytosis assay with Life-act was performed with the 100× objective.

Maximum projections of fixed images was performed using Fiji software, and vesicles were determined either counting blinded images (HeLa experiments and experiments with SKN cells overexpressing Rac^r constructs) or by CellProfiler (Carpenter et al., 2006; all other SKN experiments). Distance between cells in cell repulsion assays was measured in MetaMorph (Molecular Devices). Where stated, nearest-neighbors 2D deconvolution was performed using MetaMorph (Molecular Devices). For visualization purposes, all images are presented after intensity adjustment in Photoshop (Adobe). All adjustments within an experiment performed equally, and gamma levels were never changed.

Rac FRET Assay

Wild-type (control) HeLa cells overexpressing RaichuEV-Rac1 biosensor or coexpressing either untagged ephrinB2, or untagged EphB2 were seeded in a 3-mm glass-bottom imaging culture dish (MatTek). Cells were starved overnight before simulation. Fused ectodomains of either ephrinB2 or EphB2 were clustered as described in the Endocytosis assay with soluble Eph or ephrin ectodomains section using dyLight649 α-humanFc antibodies. Cells were imaged live before and 10 and 20 min after stimulation using an X-Cite halogen lamp (Excelitas Technologies) with 436/20×, 480/40 m (CFP), 500/20×, 535/30 m (YFP), 526/20×, 535/30 m (CFP-YFP), and 640/30×, 690/50 m filter cubes (Chroma Technology Corp.). The FRET ratio was calculated from maximum-projection images using the Fiji plugin (Fret Analyzer; http://rsb.info.nih.gov/ij/plugins/fret-analyzer/fret-analyzer.html), and total fluorescence intensity of the Fc signal was calculated using Fiji.

Image-based siRNA screen of Rho GEFs and GAPs

A list of all human proteins containing either a Dbl homology or DOCK homology domain (GEFs), as well as those containing a RhoGAP domain (GAPs), was generated by bioinformatic analysis of the UniProt database (http://www.uniprot.org). The Stealth siRNA library consisted of four separate oligonucleotides with nonoverlapping sequences per gene (Thermo Fisher Scientific and Technology Development Studio of the Max Planck Institute of Molecular Cell Biology and Genetics; see Table S1). Unique oligos were arrayed in individual wells of 96-well plates, each plate also including 4 scramble oligo wells, 3 ephrinB2-targeting wells, and 2 wells targeting both ephrinB1 and 2. The final concentration of oligonucleotides in each well was 14 nM. Each plate was assayed twice. The trans-endocytosis assay in SKN-H2B-RFP cells was performed as described in theTrans-endocytosis assay section and analysis with CellProfiler software is detailed in Fig. 2 A. A cutoff ($X \geq$ vesicles) set to contain 40% of cells from the mean scramble value for each individual plate was used to determine z-scores (see Fig. S5, A and B). Z-scores for each well were calculated at that same cutoff using the formula: (observed value − scramble mean)/scramble SD. The mean z-score per oligo was calculated and hits determined when either below −1.25 or above 1.75. Candidate genes were ranked by mean z-score for all four oligos.

Statistical analysis

Data were analyzed using Prism (GraphPad Software). Data are shown as mean ± SEM, unless stated otherwise. Statistical significance was tested with a one-way analysis of variance (ANOVA) followed by Dunnett's post hoc test, repeated measures ANOVA followed by Dunnett's or Bonferroni's post hoc test, Student's *t* test, or two-way ANOVA, where appropriate.

Online supplemental material

Fig. S1 shows the effect of Rac inhibition on actin polymerization and EphB2 trans-endocytosis and is related to Fig. 1. Fig. S2 shows further analysis and additional control experiments relating to the requirement of Rac for EphB2ΔC trans-endocytosis into ephrinB$^+$ cells and is related to Fig. 2. Fig. S3 shows additional images and analysis of the FRET data correlating EphB2 and ephrinB1 trans-endocytosis with elevated Rac activity and is related to Fig. 4. Fig. S4 is related to Fig. 5 and shows further data on the role of RhoA and Cdc42 GTPase families on EphB2-Fc endocytosis, as well as Western blot confirmation of siRNA knockdowns. Fig. S5 is related to Figs. 6 and 7 and shows control data for the siRNA screen of Rho GEFs and GAPs, as well as for the role of Tiams in EphB2ΔC trans-endocytosis. Table S1 shows complete results, including the sequences of oligos used for the siRNA screen of Rho GEFs and GAPs that is graphically displayed in Fig. 6. Videos 1 and 2

show the enrichment of actin or lack thereof after Rac inhibition at sites of EphB2ΔC trans-endocytosis and are related to Fig. 1. Videos 3 and 4 show the trans-endocytosis of EphB2ΔC into ephrinB$^+$ cortical neurons or lack thereof after Rac inhibition and are related to Fig. 3. Videos 5 and 6 show EphB2ΔC-triggered cell repulsion or lack thereof after Rac inhibition and are related to Fig. 8. Online supplemental material is available at http://www.jcb.org/cgi/content/full/jcb.201512010/DC1.

Acknowledgments

We thank Jingyi Gong, Marc Bickle, Thomas Biederer, and Angeliki Malliri for material and discussion; Chris Kuffer and Louise Gaitanos for experimental support; and Sónia Paixão, Daniel del Toro, and Laura Loschek for critically reading the manuscript.

This study was funded by the Max Planck Society and the Deutsche Forschungsgemeinschaft (Synergy).

The authors declare no competing financial interests.

Submitted: 2 December 2015
Accepted: 9 August 2016

References

Batlle, E., and D.G. Wilkinson. 2012. Molecular mechanisms of cell segregation and boundary formation in development and tumorigenesis. *Cold Spring Harb. Perspect. Biol.* 4:a008227. http://dx.doi.org/10.1101/cshperspect.a008227

Boissier, P., J. Chen, and U. Huynh-Do. 2013. EphA2 signaling following endocytosis: role of Tiam1. *Traffic.* 14:1255–1271. http://dx.doi.org/10.1111/tra.12123

Carpenter, A.E., T.R. Jones, M.R. Lamprecht, C. Clarke, I.H. Kang, O. Friman, D.A. Guertin, J.H. Chang, R.A. Lindquist, J. Moffat, et al. 2006. CellProfiler: image analysis software for identifying and quantifying cell phenotypes. *Genome Biol.* 7:R100. http://dx.doi.org/10.1186/gb-2006-7-10-r100

Cook, D.R., K.L. Rossman, and C.J. Der. 2014. Rho guanine nucleotide exchange factors: regulators of Rho GTPase activity in development and disease. *Oncogene.* 33:4021–4035. http://dx.doi.org/10.1038/onc.2013.362

Corbetta, S., S. Gualdoni, G. Ciceri, M. Monari, E. Zuccaro, V.L. Tybulewicz, and I. de Curtis. 2009. Essential role of Rac1 and Rac3 GTPases in neuronal development. *FASEB J.* 23:1347–1357. http://dx.doi.org/10.1096/fj.08-121574

Cowan, C.W., Y.R. Shao, M. Sahin, S.M. Shamah, M.Z. Lin, P.L. Greer, S. Gao, E.C. Griffith, J.S. Brugge, and M.E. Greenberg. 2005. Vav family GEFs link activated Ephs to endocytosis and axon guidance. *Neuron.* 46:205–217. http://dx.doi.org/10.1016/j.neuron.2005.03.019

Csépányi-Kömi, R., G. Sirokmány, M. Geiszt, and E. Ligeti. 2012. ARHGAP25, a novel Rac GTPase-activating protein, regulates phagocytosis in human neutrophilic granulocytes. *Blood.* 119:573–582. http://dx.doi.org/10.1182/blood-2010-12-324053

Davis, S., N.W. Gale, T.H. Aldrich, P.C. Maisonpierre, V. Lhotak, T. Pawson, M. Goldfarb, and G.D. Yancopoulos. 1994. Ligands for EPH-related receptor tyrosine kinases that require membrane attachment or clustering for activity. *Science.* 266:816–819. http://dx.doi.org/10.1126/science.7973638

Deininger, K., M. Eder, E.R. Kramer, W. Zieglgänsberger, H.U. Dodt, K. Dornmair, J. Colicelli, and R. Klein. 2008. The Rab5 guanylate exchange factor Rin1 regulates endocytosis of the EphA4 receptor in mature excitatory neurons. *Proc. Natl. Acad. Sci. USA.* 105:12539–12544. http://dx.doi.org/10.1073/pnas.0801174105

Dyer, J.O., R.S. Demarco, and E.A. Lundquist. 2010. Distinct roles of Rac GTPases and the UNC-73/Trio and PIX-1 Rac GTP exchange factors in neuroblast protrusion and migration in *C. elegans*. *Small GTPases.* 1:44–61. http://dx.doi.org/10.4161/sgtp.1.1.12991

Franke, K., W. Otto, S. Johannes, J. Baumgart, R. Nitsch, and S. Schumacher. 2012. miR-124-regulated RhoG reduces neuronal process complexity via ELMO/Dock180/Rac1 and Cdc42 signalling. *EMBO J.* 31:2908–2921. http://dx.doi.org/10.1038/emboj.2012.130

Gaitanos, T.N., R.M. Buey, J.F. Díaz, P.T. Northcote, P. Teesdale-Spittle, J.M. Andreu, and J.H. Miller. 2004. Peloruside A does not bind to the taxoid site on beta-tubulin and retains its activity in multidrug-resistant cell lines. *Cancer Res.* 64:5063–5067. http://dx.doi.org/10.1158/0008-5472.CAN-04-0771

Gong, J., R. Körner, L. Gaitanos, and R. Klein. 2016. Exosomes mediate cell contact-independent ephrin-Eph signaling during axon guidance. *J. Cell Biol.* 214:35–44. http://dx.doi.org/10.1083/jcb.201601085

Groeger, G., and C.D. Nobes. 2007. Co-operative Cdc42 and Rho signalling mediates ephrinB-triggered endothelial cell retraction. *Biochem. J.* 404:23–29. http://dx.doi.org/10.1042/BJ20070146

Gu, Y., M.D. Filippi, J.A. Cancelas, J.E. Siefring, E.P. Williams, A.C. Jasti, C.E. Harris, A.W. Lee, R. Prabhakar, S.J. Atkinson, et al. 2003. Hematopoietic cell regulation by Rac1 and Rac2 guanosine triphosphatases. *Science.* 302:445–449. http://dx.doi.org/10.1126/science.1088485

Heasman, S.J., and A.J. Ridley. 2008. Mammalian Rho GTPases: new insights into their functions from in vivo studies. *Nat. Rev. Mol. Cell Biol.* 9:690–701. http://dx.doi.org/10.1038/nrm2476

Himanen, J.P., L. Yermekbayeva, P.W. Janes, J.R. Walker, K. Xu, L. Atapattu, K.R. Rajashankar, A. Mensinga, M. Lackmann, D.B. Nikolov, and S. Dhe-Paganon. 2010. Architecture of Eph receptor clusters. *Proc. Natl. Acad. Sci. USA.* 107:10860–10865. http://dx.doi.org/10.1073/pnas.1004148107

Huber, C., A. Mårtensson, G.M. Bokoch, D. Nemazee, and A.L. Gavin. 2008. FGD2, a CDC42-specific exchange factor expressed by antigen-presenting cells, localizes to early endosomes and active membrane ruffles. *J. Biol. Chem.* 283:34002–34012. http://dx.doi.org/10.1074/jbc.M803957200

Irie, F., and Y. Yamaguchi. 2002. EphB receptors regulate dendritic spine development via intersectin, Cdc42 and N-WASP. *Nat. Neurosci.* 5:1117–1118. http://dx.doi.org/10.1038/nn964

Itoh, R.E., K. Kurokawa, Y. Ohba, H. Yoshizaki, N. Mochizuki, and M. Matsuda. 2002. Activation of rac and cdc42 video imaged by fluorescent resonance energy transfer-based single-molecule probes in the membrane of living cells. *Mol. Cell. Biol.* 22:6582–6591. http://dx.doi.org/10.1128/MCB.22.18.6582-6591.2002

Jaiswal, M., R. Dvorsky, and M.R. Ahmadian. 2013. Deciphering the molecular and functional basis of Dbl family proteins: a novel systematic approach toward classification of selective activation of the Rho family proteins. *J. Biol. Chem.* 288:4486–4500. http://dx.doi.org/10.1074/jbc.M112.429746

Jørgensen, C., A. Sherman, G.I. Chen, A. Pasculescu, A. Poliakov, M. Hsiung, B. Larsen, D.G. Wilkinson, R. Linding, and T. Pawson. 2009. Cell-specific information processing in segregating populations of Eph receptor ephrin-expressing cells. *Science.* 326:1502–1509. http://dx.doi.org/10.1126/science.1176615

Joset, A., D.A. Dodd, S. Halegoua, and M.E. Schwab. 2010. Pincher-generated Nogo-A endosomes mediate growth cone collapse and retrograde signaling. *J. Cell Biol.* 188:271–285. http://dx.doi.org/10.1083/jcb.200906089

Kaneko, T., A. Maeda, M. Takefuji, H. Aoyama, M. Nakayama, S. Kawabata, Y. Kawano, A. Iwamatsu, M. Amano, and K. Kaibuchi. 2005. Rho mediates endocytosis of epidermal growth factor receptor through phosphorylation of endophilin A1 by Rho-kinase. *Genes Cells.* 10:973–987. http://dx.doi.org/10.1111/j.1365-2443.2005.00895.x

Kania, A., and R. Klein. 2016. Mechanisms of ephrin-Eph signalling in development, physiology and disease. *Nat. Rev. Mol. Cell Biol.* 17:240–256. http://dx.doi.org/10.1038/nrm.2015.16

Khelfaoui, M., A. Pavlowsky, A.D. Powell, P. Valnegri, K.W. Cheong, Y. Blandin, M. Passafaro, J.G. Jefferys, J. Chelly, and P. Billuart. 2009. Inhibition of RhoA pathway rescues the endocytosis defects in Oligophrenin1 mouse model of mental retardation. *Hum. Mol. Genet.* 18:2575–2583. http://dx.doi.org/10.1093/hmg/ddp189

Klein, R. 2012. Eph/ephrin signalling during development. *Development.* 139:4105–4109. http://dx.doi.org/10.1242/dev.074997

Kullander, K., S.D. Croll, M. Zimmer, L. Pan, J. McClain, V. Hughes, S. Zabski, T.M. DeChiara, R. Klein, G.D. Yancopoulos, and N.W. Gale. 2001. Ephrin-B3 is the midline barrier that prevents corticospinal tract axons from recrossing, allowing for unilateral motor control. *Genes Dev.* 15:877–888. http://dx.doi.org/10.1101/gad.868901

Lauterbach, J., and R. Klein. 2006. Release of full-length EphB2 receptors from hippocampal neurons to cocultured glial cells. *J. Neurosci.* 26:11575–11581. http://dx.doi.org/10.1523/JNEUROSCI.2697-06.2006

Lisabeth, E.M., G. Falivelli, and E.B. Pasquale. 2013. Eph receptor signaling and ephrins. *Cold Spring Harb. Perspect. Biol.* 5:a009159. http://dx.doi.org/10.1101/cshperspect.a009159

Marchesi, S., F. Montani, G. Deflorian, R. D'Antuono, A. Cuomo, S. Bologna, C. Mazzoccoli, T. Bonaldi, P.P. Di Fiore, and F. Nicassio. 2014. DEP DC1B coordinates de-adhesion events and cell-cycle progression at

mitosis. *Dev. Cell.* 31:420–433. http://dx.doi.org/10.1016/j.devcel.2014.09.009

Marston, D.J., S. Dickinson, and C.D. Nobes. 2003. Rac-dependent trans-endocytosis of ephrinBs regulates Eph-ephrin contact repulsion. *Nat. Cell Biol.* 5:879–888. http://dx.doi.org/10.1038/ncb1044

Nakano-Kobayashi, A., N.N. Kasri, S.E. Newey, and L. Van Aelst. 2009. The Rho-linked mental retardation protein OPHN1 controls synaptic vesicle endocytosis via endophilin A1. *Curr. Biol.* 19:1133–1139. http://dx.doi.org/10.1016/j.cub.2009.05.022

Nakaya, M., M. Tanaka, Y. Okabe, R. Hanayama, and S. Nagata. 2006. Opposite effects of rho family GTPases on engulfment of apoptotic cells by macrophages. *J. Biol. Chem.* 281:8836–8842. http://dx.doi.org/10.1074/jbc.M510972200

Negrete, O.A., E.L. Levroney, H.C. Aguilar, A. Bertolotti-Ciarlet, R. Nazarian, S. Tajyar, and B. Lee. 2005. EphrinB2 is the entry receptor for Nipah virus, an emergent deadly paramyxovirus. *Nature.* 436:401–405. http://dx.doi.org/10.1038/nature03838

Nishimura, T., T. Yamaguchi, A. Tokunaga, A. Hara, T. Hamaguchi, K. Kato, A. Iwamatsu, H. Okano, and K. Kaibuchi. 2006. Role of numb in dendritic spine development with a Cdc42 GEF intersectin and EphB2. *Mol. Biol. Cell.* 17:1273–1285. http://dx.doi.org/10.1091/mbc.E05-07-0700

Parker, M., R. Roberts, M. Enriquez, X. Zhao, T. Takahashi, D. Pat Cerretti, T. Daniel, and J. Chen. 2004. Reverse endocytosis of transmembrane ephrin-B ligands via a clathrin-mediated pathway. *Biochem. Biophys. Res. Commun.* 323:17–23. http://dx.doi.org/10.1016/j.bbrc.2004.07.209

Pasquale, E.B. 2008. Eph-ephrin bidirectional signaling in physiology and disease. *Cell.* 133:38–52. http://dx.doi.org/10.1016/j.cell.2008.03.011

Pasquale, E.B. 2010. Eph receptors and ephrins in cancer: bidirectional signalling and beyond. *Nat. Rev. Cancer.* 10:165–180. http://dx.doi.org/10.1038/nrc2806

Pernet, O., C. Pohl, M. Ainouze, H. Kweder, and R. Buckland. 2009. Nipah virus entry can occur by macropinocytosis. *Virology.* 395:298–311. http://dx.doi.org/10.1016/j.virol.2009.09.016

Qin, H., R. Noberini, X. Huan, J. Shi, E.B. Pasquale, and J. Song. 2010. Structural characterization of the EphA4-Ephrin-B2 complex reveals new features enabling Eph-ephrin binding promiscuity. *J. Biol. Chem.* 285:644–654. http://dx.doi.org/10.1074/jbc.M109.064824

Riedl, J., A.H. Crevenna, K. Kessenbrock, J.H. Yu, D. Neukirchen, M. Bista, F. Bradke, D. Jenne, T.A. Holak, Z. Werb, et al. 2008. Lifeact: a versatile marker to visualize F-actin. *Nat. Methods.* 5:605–607. http://dx.doi.org/10.1038/nmeth.1220

Roberts, P.J., N. Mitin, P.J. Keller, E.J. Chenette, J.P. Madigan, R.O. Currin, A.D. Cox, O. Wilson, P. Kirschmeier, and C.J. Der. 2008. Rho Family GTPase modification and dependence on CAAX motif-signaled posttranslational modification. *J. Biol. Chem.* 283:25150–25163. http://dx.doi.org/10.1074/jbc.M800882200

Rooney, C., G. White, A. Nazgiewicz, S.A. Woodcock, K.I. Anderson, C. Ballestrem, and A. Malliri. 2010. The Rac activator STEF (Tiam2) regulates cell migration by microtubule-mediated focal adhesion disassembly. *EMBO Rep.* 11:292–298. http://dx.doi.org/10.1038/embor.2010.10

Sahin, M., P.L. Greer, M.Z. Lin, H. Poucher, J. Eberhart, S. Schmidt, T.M. Wright, S.M. Shamah, S. O'connell, C.W. Cowan, et al. 2005. Eph-dependent tyrosine phosphorylation of ephexin1 modulates growth cone collapse. *Neuron.* 46:191–204. http://dx.doi.org/10.1016/j.neuron.2005.01.030

Schaupp, A., O. Sabet, I. Dudanova, M. Ponserre, P. Bastiaens, and R. Klein. 2014. The composition of EphB2 clusters determines the strength in the cellular repulsion response. *J. Cell Biol.* 204:409–422. http://dx.doi.org/10.1083/jcb.201305037

Schindelin, J., I. Arganda-Carreras, E. Frise, V. Kaynig, M. Longair, T. Pietzsch, S. Preibisch, C. Rueden, S. Saalfeld, B. Schmid, et al. 2012. Fiji: an open-source platform for biological-image analysis. *Nat. Methods.* 9:676–682. http://dx.doi.org/10.1038/nmeth.2019

Seiradake, E., K. Harlos, G. Sutton, A.R. Aricescu, and E.Y. Jones. 2010. An extracellular steric seeding mechanism for Eph-ephrin signaling platform assembly. *Nat. Struct. Mol. Biol.* 17:398–402. http://dx.doi.org/10.1038/nsmb.1782

Seiradake, E., D. del Toro, D. Nagel, F. Cop, R. Härtl, T. Ruff, G. Seyit-Bremer, K. Harlos, E.C. Border, A. Acker-Palmer, et al. 2014. FLRT structure: balancing repulsion and cell adhesion in cortical and vascular development. *Neuron.* 84:370–385. http://dx.doi.org/10.1016/j.neuron.2014.10.008

Shamah, S.M., M.Z. Lin, J.L. Goldberg, S. Estrach, M. Sahin, L. Hu, M. Bazalakova, R.L. Neve, G. Corfas, A. Debant, and M.E. Greenberg. 2001. EphA receptors regulate growth cone dynamics through the novel guanine nucleotide exchange factor ephexin. *Cell.* 105:233–244. http://dx.doi.org/10.1016/S0092-8674(01)00314-2

Shutes, A., C. Onesto, V. Picard, B. Leblond, F. Schweighoffer, and C.J. Der. 2007. Specificity and mechanism of action of EHT 1864, a novel small molecule inhibitor of Rac family small GTPases. *J. Biol. Chem.* 282:35666–35678. http://dx.doi.org/10.1074/jbc.M703571200

Smyth, J.W., J.M. Vogan, P.J. Buch, S.S. Zhang, T.S. Fong, T.T. Hong, and R.M. Shaw. 2012. Actin cytoskeleton rest stops regulate anterograde traffic of connexin 43 vesicles to the plasma membrane. *Circ. Res.* 110:978–989. http://dx.doi.org/10.1161/CIRCRESAHA.111.257964

Swanson, J.A. 2008. Shaping cups into phagosomes and macropinosomes. *Nat. Rev. Mol. Cell Biol.* 9:639–649. http://dx.doi.org/10.1038/nrm2447

Takeuchi, S., H. Katoh, and M. Negishi. 2015. Eph/ephrin reverse signalling induces axonal retraction through RhoA/ROCK pathway. *J. Biochem.* 158:245–252. http://dx.doi.org/10.1093/jb/mvv042

Tanaka, M., R. Ohashi, R. Nakamura, K. Shinmura, T. Kamo, R. Sakai, and H. Sugimura. 2004. Tiam1 mediates neurite outgrowth induced by ephrin-B1 and EphA2. *EMBO J.* 23:1075–1088. http://dx.doi.org/10.1038/sj.emboj.7600128

Tcherkezian, J., and N. Lamarche-Vane. 2007. Current knowledge of the large RhoGAP family of proteins. *Biol. Cell.* 99:67–86. http://dx.doi.org/10.1042/BC20060086

Terawaki, S., K. Kitano, T. Mori, Y. Zhai, Y. Higuchi, N. Itoh, T. Watanabe, K. Kaibuchi, and T. Hakoshima. 2010. The PHCCEx domain of Tiam1/2 is a novel protein- and membrane-binding module. *EMBO J.* 29:236–250. http://dx.doi.org/10.1038/emboj.2009.323

Tolias, K.F., J.B. Bikoff, C.G. Kane, C.S. Tolias, L. Hu, and M.E. Greenberg. 2007. The Rac1 guanine nucleotide exchange factor Tiam1 mediates EphB receptor-dependent dendritic spine development. *Proc. Natl. Acad. Sci. USA.* 104:7265–7270. http://dx.doi.org/10.1073/pnas.0702044104

Um, K., S. Niu, J.G. Duman, J.X. Cheng, Y.K. Tu, B. Schwechter, F. Liu, L. Hiles, A.S. Narayanan, R.T. Ash, et al. 2014. Dynamic control of excitatory synapse development by a Rac1 GEF/GAP regulatory complex. *Dev. Cell.* 29:701–715. http://dx.doi.org/10.1016/j.devcel.2014.05.011

Wennerberg, K., S.M. Ellerbroek, R.Y. Liu, A.E. Karnoub, K. Burridge, and C.J. Der. 2002. RhoG signals in parallel with Rac1 and Cdc42. *J. Biol. Chem.* 277:47810–47817. http://dx.doi.org/10.1074/jbc.M203816200

Xu, N.J., and M. Henkemeyer. 2009. Ephrin-B3 reverse signaling through Grb4 and cytoskeletal regulators mediates axon pruning. *Nat. Neurosci.* 12:268–276. http://dx.doi.org/10.1038/nn.2254

Xu, Q., and D.G. Wilkinson. 2013. Boundary formation in the development of the vertebrate hindbrain. *Wiley Interdiscip. Rev. Dev. Biol.* 2:735–745. http://dx.doi.org/10.1002/wdev.106

Yoo, S., J. Shin, and S. Park. 2010. EphA8-ephrinA5 signaling and clathrin-mediated endocytosis is regulated by Tiam-1, a Rac-specific guanine nucleotide exchange factor. *Mol. Cells.* 29:603–609. http://dx.doi.org/10.1007/s10059-010-0075-2

Zhuang, G., S. Hunter, Y. Hwang, and J. Chen. 2007. Regulation of EphA2 receptor endocytosis by SHIP2 lipid phosphatase via phosphatidylinositol 3-Kinase-dependent Rac1 activation. *J. Biol. Chem.* 282:2683–2694. http://dx.doi.org/10.1074/jbc.M608509200

Zimmer, M., A. Palmer, J. Köhler, and R. Klein. 2003. EphB-ephrinB bi-directional endocytosis terminates adhesion allowing contact mediated repulsion. *Nat. Cell Biol.* 5:869–878. http://dx.doi.org/10.1038/ncb1045